Paper

エチレンジアミン四酢酸誘導体を用いた銀析出型エレクトロクロミックデバイスにおける銀ナノ粒子の電気化学的形態制御

宇治 駿、梅谷 虎太郎、Nikhil C. Bhoumik、中村 一希、
Christopher J. Barile、小林 範久

要旨　銀ナノ粒子(AgNPs)は、その形態によって様々な色彩色を示すことができる。本研究では、エチレンジアミン四酢酸(EDTA)の誘導体を利用して、Ag析出ベースのエレクトロクロミック(EC)デバイスにおけるAgNPsの電着モルフォロジーを制御した。EDTA誘導体のカルボキシル基は電気化学的にラジカルアニオンに還元され、電気化学的メディエーターとして働くため、AgNPの析出が促進された。その結果、析出したAgNPの形態は、EDTA誘導体の媒介効果により、棒や針のような異方的な形状を形成した。さらに、EDTA誘導体を用いたECデバイスは、AgNPが多孔質構造として形成され、多重散乱を誘起するため、深い黒色状態を示した。その結果、ITOナノ粒子修飾電極を用いない場合、20%以下の反射率の平坦電極上で黒色状態が達成された。

キーワード：エレクトロクロミズム、調光窓、銀、電着、電気化学メディエーター、貴金属ナノ粒子

1. はじめに

エレクトロクロミック(EC)現象は、電極への電子移動によるEC材料の電子状態の変化を伴い、可逆的な光学的変化をもたらす。[1) 4)] 有機および無機物質を含むEC材料については、数多くの研究がなされている。[5) 12)] EC技術を組み込んだデバイスは、自己発光ディスプレイ、低い動作電圧、色の保持、太陽光下での高い視認性などに比べていくつかの利点がある、ECデバイスは、電子紙、デジタルサイネージ、スマートウィンドウなどの情報ディスプレイや光変調デバイスへの応用が期待されている[16) 22)]。

様々なEC材料の中でも、無機EC材料は電気化学的安定性と実用化により、大きな注目を集めている。これらの無機EC材料は、2つのタイプに分類することができる。第一のタイプの無機EC材料は、WO_3、NiO、MnO_2を含む遷移金属酸化物からなる。[23) 28)] 外部電圧によってこれらの金属酸化物薄膜の価数状態が変化すると、H^+やLi^+のようなイオン半径の小さい陽イオンが電荷補償のために結晶格子に挿入され、色調の変化を引き起こす。第二のタイプは、Ag、Bi、Cu、Znなどの可逆的な電着が可能な金属を含む[29) 39)] これらのEC系では、金属ミラー、黒、白などの無彩色がEC電解質溶液に溶解した金属陽イオンとして現れ、透明な導電性電極上で還元と電着を受ける。

フルカラーECデバイスの開発には、1画素内で安定したマルチカラー表現が可能なシンプルな構造が必要である。しかし、有機EC材料とは異なり、無機EC材料で多色化を達成することは、多段階の酸化還元反応が複雑であるため、依然として困難である。この制限を克服するために、我々のこれまでの研究では、銀ナノ粒子(AgNP)の電着と溶解を利用して、無彩色から有彩色までの明瞭な光学状態を達成するECデバイスを発表した[35)40) 47)]。そのデフォルト状態では、デバイスは透明のままであるが、負電圧を印加すると電極表面にAgNP電着が誘発される。この多色化を可能にする重要なメカニズムは、インジウムスズ酸化物(ITO)電極のような透明電極上に電着したAgNPsを形態学的に制御することから導き出された。

Received March 22, 2025; Revised May 24, 2025; Accepted July 2, 2025
†1 Graduate School of Engineering, Chiba University
(Chiba, Japan)
†2 Graduate School of Engineering, Tokyo Polytechnic University
(Kanagawa, Japan)
†3 Department of Chemistry, University of Nevada, Reno

Paper

Electrochemical Morphology Control of Silver Nanoparticles in Silver Deposition-Based Electrochromic Devices Employing a Derivative of Ethylenediaminetetraacetic Acid

Shun Uji[†1, †2], Kotaro Umetani[†1], Nikhil C. Bhoumik[†3], Kazuki Nakamura[†1], Christopher J. Barile[†3] and Norihisa Kobayashi[†1]

Abstract Silver nanoparticles (AgNPs) can exhibit various chromatic colorations depending on their morphology. This study utilized a derivative of ethylenediaminetetraacetic acid (EDTA) to control the electrodeposited morphology of AgNPs in an Ag deposition-based electrochromic (EC) device. Because the carboxyl groups of the EDTA derivative were electrochemically reduced to radical anion and worked as an electrochemical mediator, the deposition of AgNPs was promoted. As a result, the morphology of deposited AgNPs formed an anisotropic shape, such as a rod or needle, due to the mediation effect of the EDTA derivative. Moreover, the EC device with EDTA derivative exhibited a deep black state since AgNPs were formed as porous structures, inducing multiple scattering. Consequently, a black state on a flat electrode with less than 20% reflection was achieved without the ITO nanoparticles-modified electrode.

Keywords: Electrochromism, Dynamic window, Silver, Electrodeposition, Electrochemical mediation, Noble metal nanoparticles.

1. Introduction

The electrochromic (EC) phenomenon involves a change in the electronic state of the EC material due to electron transfer to the electrode, leading to reversible optical changes.[1)~4)] Numerous studies have explored EC materials, including organic and inorganic substances.[5)~12)] Devices incorporating EC technology offer several advantages over self-emissive displays, low operating voltages, color retention, high visibility under sunlight, etc.[13)~15)] Due to these advantages, EC devices are considered promising for applications in information displays and light-modulating devices, such as electronic paper, digital signage, and smart windows.[16)~22)]

Among various EC materials, inorganic EC materials have gained significant attention because of their electrochemical stability and practical applications. These inorganic EC materials can be categorized into two types. The first type of inorganic EC materials consists of transition metal oxides, including WO_3, NiO, and MnO_2.[23)~28)] When an external voltage alters the valence state of these metal oxide films, cations with small ionic radii, such as H^+ and Li^+, are inserted into the crystal lattice for charge compensation, causing a change in coloration. The second type includes metals capable of reversible electrodeposition, such as Ag, Bi, Cu, and Zn.[29)~39)] In these EC systems, achromatic colors, including metallic mirrors, black, and white, appear as metal cations dissolved in the EC electrolyte solution and undergo reduction and electrodeposition onto a transparent conductive electrode.

Developing a full-color EC device requires a simple structure capable of stable multi-color representation within a single pixel. However, unlike organic EC materials, achieving multi-coloration with inorganic EC materials remains challenging owing to the complexity of multi-step redox reactions. To overcome this limitation, our previous studies have presented an EC device that utilizes the electrodeposition and dissolution of silver nanoparticles (AgNPs) to achieve distinct optical states ranging from achromatic to chromatic colors.[35)40)~47)] In its default state, the device remains transparent, while applying a negative voltage triggers AgNP electrodeposition on the electrode surface. The key mechanism enabling this multi-coloration was derived from the morphological control of the electrodeposited

Received March 22, 2025; Revised May 24, 2025; Accepted July 2, 2025
†1 Graduate School of Engineering, Chiba University (Chiba, Japan)
†2 Graduate School of Engineering, Tokyo Polytechnic University (Kanagawa, Japan)
†3 Department of Chemistry, University of Nevada, Reno (Nevada, USA)

AgNPsのクロマチックカラーリングは、局在表面プラズモン共鳴(LSPR)として知られるプラズモニック現象による光吸収に起因する。LSPRバンドの波長は、金属ナノ粒子のサイズと形状に基づいてシフトする。[48) 50)] その結果、LSPRバンドを制御するためにITO電極上に電着AgNPの形態を調整することで、大きな色の変化を達成することができる。このAg析出ベースのECデバイスは、Ag^+イオンを含むECゲル電解質溶液のみからなるシンプルな構造を特徴とし、一対のITO電極の間に挟まれている。注目すべきは、このECデバイスは、電着AgNPの素直な電気化学的析出と溶解による色スイッチングを可能にし、10,000サイクル以上の安定性を維持していることである[35)51)]。

これまでの研究で報告されているAg蒸着ベースのECデバイスは、様々な電圧印加方法によって球状粒子の密度とサイズを制御することで、様々な着色を実現している。このECデバイスの動作は、AgNPの凝集に依存して蒸着形態に異方性を導入し、LSPRバンドの制御を可能にしている[40)43)]。しかし、AgNPの凝集は鏡面反射を増加させ、明るさと色の純度を低下させる。Ag蒸着ベースのECデバイスにおいて、色の変化をさらに拡大し、色純度を向上させるためには、凝集を最小限に抑えながら、サイズと形状を精密に制御した単離AgNPから色を得ることが不可欠である。我々の以前の研究では、AgNPsの析出形態を制御するために、Ag析出ベースのECデバイスにAg析出剤であるポリビニルピロリドン(PVP)を導入した[52),53)]。PVP分子は電着したAgNPsの表面に吸収され、凝集や過剰な成長を防ぎ、その結果、非常に明るい色と新規な着色効果をもたらす。これらの研究により、AgNPの形態とECデバイスの光学的状態を制御するキャッピング剤の有効性が実証された。しかし、蒸着されたAgNPは球状のままであったため、正確なLSPRバンド制御に必要な異方性を導入する能力が制限された。

この原稿はエチレンジアミン四酢酸(EDTA、図1(a))に焦点を当てた。これまでの研究で、EDTAが化学合成において棒状でナノワイヤー状の異方性貴金属ナノ粒子の形成を促進することが報告されている[54)]。本研究の実験では、EDTAの代わりに、プロピル主鎖が伸長したEDTAの誘導体である1,3-ジアミノプロパン-N, N, N', N'-四酢酸(DPTA、図1(b))を用いた。

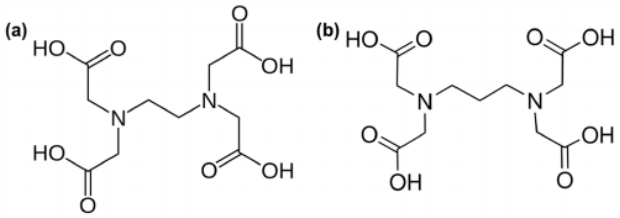

図1 (a): EDTAと(b): DPTAの構造式。

EDTAと比較して、DPTAは誘電特性が低く、有機溶媒への溶解性が向上し、DMSOをベースとしたEC電解質溶液に適している。本研究では、DPTAを組み込むことで、Ag 堆積ベースの EC デバイスの電着 AgNP に異方性を導入することを目的とした。ECデバイスの電気化学的特性とAgNPsのモルフォロジーを分析することにより、AgNPsのモルフォロジーを制御するDPTAの役割が実証された。電気化学系において、DPTAのみを添加することで異方性AgNPsを形成できるとする。この場合、AgNPsのモルフォロジー制御のさらなる進歩と、Ag蒸着ベースのECデバイスの色特性の改善が期待できる。

2実験セクション

2.1 材料

硝酸銀(I)($AgNO_3$ 、富士フイルム和光純薬、日本)、塩化銅(II)($CuCl_2$ 、関東化学株式会社、日本)、塩化リチウム(LiCl、関東化学株式会社、日本)、ジメチルスルホキシド(DMSO、Sigma Aldrich、日本)、1,3ジアミノプロパン-N、N、N'、N'-四酢酸(DPTA、Sigma-Aldrich、米国)、エチレンジアミン四酢酸(EDTA、関東化学株式会社、日本)、ヒドロキシエチレンジアミン三酢酸(HEDTA、関東化学株式会社、日本)、とポリビニルブチラル(PVB, B60T, M_w = 5.5 × 10^4, 倉原理化学会.Ltd.、日本)をそのまま使用した。洗浄後、オゾン処理したITOコートガラス基板(厚さ720μm、4.2Ω/)を使用した。2.2 EC電解質溶液の調製

DPTAの導入効果を確認するために、いくつかの電解質溶液を調製した。EC電解質溶液は、EC材料として50 mM $AgNO_3$、支持電解質として5.0 mM DPTA、250 mM LiClを溶解し、3電極ECデバイス用に調製した。さらに、5.0 mM DPTA、EDTA、またはHEDTAに250 mMのLiClをDMSOに添加して電解質溶液を調製した。

AgNPs on a transparent electrode, such as an indium tin oxide (ITO) electrode. Chromatic colorations of AgNPs result from light absorption caused by a plasmonic phenomenon known as localized surface plasmon resonance (LSPR). The wavelength of the LSPR band shifts based on the size and shape of the metal nanoparticles.[48)~50)] Consequently, significant color changes can be achieved by adjusting the morphology of electrodeposited AgNPs on the ITO electrode to control the LSPR bands. This Ag deposition-based EC device features a simple structure, consisting solely of an EC gel electrolyte solution containing Ag^+ ions sandwiched between a pair of ITO electrodes. Notably, this EC device enables color switching through straightforward electrochemical deposition and dissolution of electrodeposited AgNPs, maintaining stability over ten thousand cycles.[35)51)]

Ag deposition-based EC devices reported in previous studies have achieved various colorations by controlling the density and size of spherical particles through varying voltage application methods. This EC device operation relies on the aggregation of AgNPs to introduce anisotropy into the deposited morphology, enabling control of the LSPR band.[40)43)] However, aggregation of the AgNPs increases specular reflection and reduces the brightness and color purity. To further expand color variation and improve color purity in Ag deposition-based EC devices, it is essential to obtain the coloration from isolated AgNPs with precisely controlled size and shape while minimizing aggregation. Our previous study introduced polyvinylpyrrolidone (PVP), a capping agent for AgNPs, into an Ag deposition-based EC device to control the deposition morphology of AgNPs.52),53) PVP molecules are absorbed onto the surface of electrodeposited AgNPs, preventing aggregation and excessive growth, resulting in highly bright colors and novel coloration effects. These studies demonstrated the effectiveness of capping agents in controlling AgNP morphology and the optical state of the EC device. However, the deposited AgNPs remained spherical, limiting the ability to introduce the anisotropy necessary for precise LSPR band control.

This manuscript focused on ethylenediaminetetraacetic acid (EDTA, Fig. 1(a)). Previous studies have reported that EDTA promoted the formation of rod-shaped and nanowire-like anisotropic noble metal nanoparticles in chemical synthesis.[54)] For the experiments in this study, 1,3-diaminopropane-N, N, N', N'-tetraacetic acid (DPTA, Fig. 1(b)), a derivative of EDTA with an extended propyl

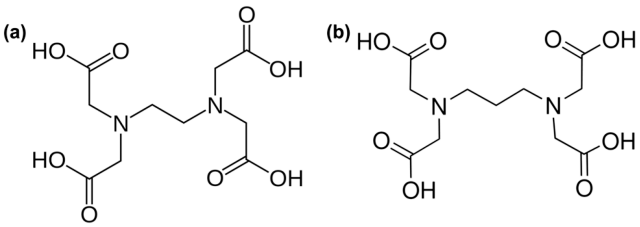

Fig. 1 The structural formulas of (a): EDTA and (b): DPTA.

main chain, was used instead of EDTA. Compared to EDTA, DPTA has a lower dielectric property, enhancing its solubility in organic solvents and making it more suitable for our EC electrolyte solutions based on DMSO. This study aimed to introduce anisotropy into electrodeposited AgNPs in Ag deposition-based EC devices by incorporating DPTA. By analyzing the electrochemical properties of the EC device and the morphology of the AgNPs, the role of DPTA in controlling the morphology of AgNPs was demonstrated. Suppose anisotropic AgNPs can be formed in an electrochemical system by adding only DPTA. In that case, further advancements in morphology control of AgNPs and improvements in the coloration properties of Ag deposition-based EC devices can be expected.

2. Experimental Section

2.1 Materials

Silver(I) nitrate ($AgNO_3$, FUJIFILM Wako Pure Chemical Corporation, Japan), copper(II) chloride ($CuCl_2$, Kanto Chemical Co., Inc., Japan), lithium chloride (LiCl, Kanto Chemical Co., Inc., Japan), dimethyl sulfoxide (DMSO, Sigma Aldrich, Japan), 1,3-diamino propane-N, N, N', N'-tetraacetic acid (DPTA, Sigma-Aldrich, U.S.A), ethylenediaminetetraacetic acid (EDTA, Kanto Chemical Co., Inc., Japan), hydroxyethylenediaminetriacetic acid (HEDTA, Kanto Chemical Co., Inc., Japan), and polyvinyl butyral (PVB, B60T, $M_w = 5.5 \times 10^4$, Kuraray Co. Ltd, Japan) were used as received. ITO-coated glass substrates 720 μm thick (4.2 Ω/□) were used after washing and ozonation.

2.2 Preparation of the EC electrolyte solutions

Several electrolyte solutions were prepared to confirm the effect of the introduction of DPTA. The EC electrolyte solution was prepared for three-electrode EC devices by dissolving 50 mM $AgNO_3$ as the EC material, 5.0 mM DPTA, and 250 mM LiCl as the supporting electrolyte. In addition, electrolyte solutions were prepared by adding 5.0 mM DPTA, EDTA, or HEDTA with 250 mM of LiCl in DMSO. In the case of the two-

2電極ECデバイスの場合、3電極ECデバイス用の上記EC電解質溶液に、対反応材料および電気化学メディエーターとして10 mM $CuCl_2$を添加した。その後、10 wt.%のPVBを混合し、2電極ECデバイス用のゲルEC電解質溶液を調製した。

2.3 ECデバイスの作製

DPTAを含むEC電解質溶液の電気化学的特性および析出したAgNPの形態を調べるために、3電極ECデバイスを使用した。ITO電極を作用電極、Ptワイヤーを対極、Ag/Ag^+を参照電極として、3電極Ag析出ベースのECデバイスを作製した。ECデバイスは、3種類の電極と各電解質溶液を1cm×1cmの光学セルに配置することで作製した。また、着色特性を評価するために、より実用的なタイプの2電極ECデバイスを使用した。ゲル電解質を2つのITO電極で挟むことにより、2電極Ag析出ベースのECデバイスを作製した。このECデバイスの有効電極面積を1cm×1cmとし、スペーサーを用いて電極間の距離を300μmに維持した。

2.4 装置 ECデバイスに電圧を印加するためにポテンショスタット/ガルバノスタット(ALS/CHI 660A、ALS株式会社、日本)を使用した。参照電極は、イオン透過性ガラス(BAS、日本)を塗布したサンプルホルダーにAg^+溶液(アセトニトリル中10 mM $AgNO_3$および100 mM TBAP)を注入し、Agワイヤーを含むキャップでホルダーを封止することにより作製した。透過スペクトルおよび反射スペクトルは、ダイオードアレイ検出システム(USB4000、海洋インサイト、日本)とタングステンハロゲンランプ(HL-2000-LL、海洋インサイト、日本)を光源として記録した。電圧印加前のECデバイスの透過率スペクトルをリファレンスとして使用した。鏡面反射率標準物質(STANSSH; Ocean Insight, Japan)を 100 % 反射率基準として使用した。水晶振動子マイクロバランス(QCM)測定は、Aポテンショスタット/ガルバノスタット(ALS/CHI 440A、ALS株式会社、日本)を用いて行った。作業/参照電極または対/参照電極の電極電位は、2つのポテンショスタット(ALS/CHI 660A、ALS株式会社、日本、HAG1232m、北都電工)を用いて記録した。作用電極上に電着したAgNPsの形態を電界放出型走査電子顕微鏡(FE-SEM; JSM6510, JEOL, Japan)を用いて観察した。

3. 結果および考察

まず、DPTAを含むAg析出ベースのECデバイスの電気化学的特性を調べた。図 2(a)に、3 電極 EC 素子のサイクリックボルタンモグラム(CV)とそれに対応する 600 nm における透過率の変化を示す。DPTAを用いないECデバイスのCV(図2(a)、黒線)では、以下のところから還元電流が観測された。

-1.2V、電極上へのAgNPの電着による透過率の低下を伴う。同様に、DPTAを含むECデバイス(図2(a)、赤線)でも、Ag^+イオン還元の臨界電位は-1.2 Vで観測された。電位掃引中の光学的変化については、DPTAを用いたECデバイスが到達した最小透過率は10%以下であった。一方、DPTAを用いないデバイスの透過率は約25%に低下したのみであった。

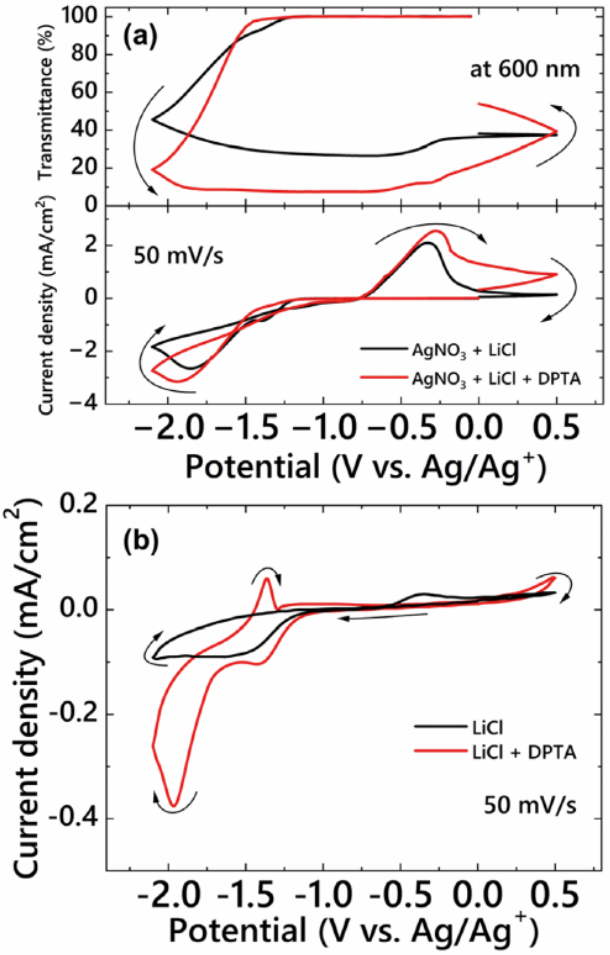

図2 3電極電気化学デバイス(a:$AgNO_3$含有、b:$AgNO_3$を除く)のDPTA有無による600nmでの透過率(上)とCV(下)の変化。

electrode EC device, 10 mM $CuCl_2$ was added to the above EC electrolyte solution for the three-electrode EC device as the counter-reaction material and electrochemical mediator. Subsequently, 10 wt.% of PVB was mixed to prepare the gel EC electrolyte solution for the two-electrode EC device.

2.3 Fabrication of the EC device

Three-electrode EC devices were used to examine the electrochemical properties of the EC electrolyte solutions containing DPTA and the morphology of deposited AgNPs. A three-electrode Ag deposition-based EC device was prepared using an ITO electrode as the working electrode, a Pt wire as the counter electrode, and Ag/Ag^+ as the reference electrode. The EC devices were fabricated by placing three kinds of electrodes and each electrolyte solution into a 1 cm × 1 cm optical cell. Two-electrode EC devices with more practical types were also used to evaluate the coloration property. A two-electrode Ag deposition-based EC device was fabricated by sandwiching a gel electrolyte between two ITO electrodes. The effective electrode area of this EC device was set to 1 cm × 1 cm, and the distance between the electrodes was maintained at 300 μm using a spacer.

2.4 Apparatus

A potentiostat/galvanostat (ALS/CHI 660A, ALS Co., Ltd., Japan) was used to apply voltage to the EC device. The reference electrode was prepared by injecting an Ag^+ solution (10 mM $AgNO_3$ and 100 mM TBAP in acetonitrile) into a sample holder with ion-permeable glass (BAS, Japan) and then sealing the holder with a cap containing an Ag wire. Transmission and reflection spectra were recorded using a diode array detection system (USB4000, Ocean Insight, Japan) and a tungsten-halogen lamp (HL-2000-LL, Ocean Insight, Japan) as the light source. The transmittance spectra of the EC device before the voltage application were used as references. A specular reflectance standard (STAN-SSH; Ocean Insight, Japan) was used as a 100 % reflectivity reference. The quartz crystal microbalance (QCM) measurement was conducted using A potentiostat/galvanostat (ALS/CHI 440A, ALS Co., Ltd., Japan). The electrode potentials of the working/reference or counter/reference electrodes were recorded using two potentiostats (ALS/CHI 660A, ALS Co., Ltd., Japan, and HAG1232m, HOKUTO DENKO, Japan). The morphology of the AgNPs electrodeposited on the working electrode was observed using field-emission scanning electron microscopy (FE-SEM; JSM-6510, JEOL, Japan).

3. Results and Discussion

First, the electrochemical properties of the Ag deposition-based EC device containing DPTA were investigated. The cyclic voltammogram (CV) and the corresponding changes in transmittance at 600 nm for the three-electrode EC device are presented in Fig. 2(a). In the CV of the EC device without DPTA (Fig. 2(a), black line), a reductive current was observed starting at –1.2 V, accompanied by a decrease in transmittance due to the electrodeposition of AgNPs on the electrode. Similarly, in the EC device containing DPTA (Fig. 2(a), red line), the critical potential for Ag^+ ion reduction was also observed at –1.2 V. Regarding the optical changes during the potential sweep, the minimum transmittance reached by the EC device with DPTA was below 10%. In contrast, the transmittance of the device without DPTA only decreased to approximately 25%. Fig. S1 presents the transmission spectra at –2.1 V (negative potential

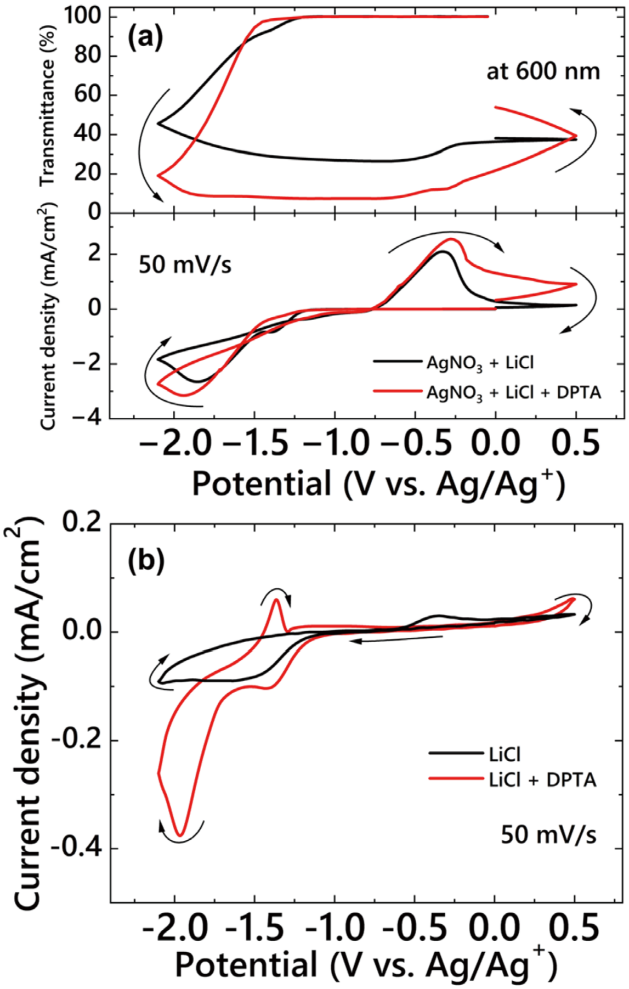

Fig. 2 Change in transmittance at 600 nm (top) and CV (bottom) of the three-electrode electrochemical devices (a: containing $AgNO_3$ and b: excluding $AgNO_3$) with or without DPTA.

図S1は、CV測定中の-2.1 V(正方向へ戻るための負の電位端)と-1.0 V(正方向への前方掃引)における透過スペクトルを示している。透過スペクトルはブロードであり、透過率の波長依存性は観察されなかった。さらに、図2(a)に示すように、DPTAを含むECデバイスの最小透過率は、DPTAを含まないデバイスの最小透過率よりも低かった。これらの結果から、DPTAがECデバイスの色調挙動に影響を与えることが示唆された。

EDTAとDPTAは金属陽イオンと錯体種を形成する金属キレート剤としてよく知られている。そこで、EC電解質溶液中でDPTAがAg^+イオンと錯体種を形成するかどうかを調べるために、電位差滴定を行った。これまでの研究から、EC電解質溶液中のAg^+イオンは、支持電解質(本研究ではCl^-イオン)のハロゲン化物イオンと複合種を形成する。10mMの$AgNO_3$と50mMのLiClをDMSOに溶解し、$AgCl_n^{(n-1)-}$を含む10mL溶液を調製した。次に、$AgCl_n^{(n-1)-}$溶液に25 mM DPTAを含むDMSO溶液を徐々に添加しながら平衡電位を測定した。電解液中のAg/Ag^+酸化還元反応の平衡電極電位は、AgSワイヤーを指示電極とし、Ag/Ag^+参照電極を用いて測定した。AgCl n(n-1)- を含む電解液に DPTA 溶液を徐々に添加し、自発電位変化(図 S2)をモニターした。DPTA添加前の平衡電位は-0.65 V(vs. Ag/Ag^+)であった。電位を測定しながら、DPTA溶液を合計20mLずつ段階的に導入した。その結果、平衡電極電位は、DPTA溶液を20 mL添加しても、-0.64 V付近でほぼ安定したままであった。20mLのDPTA溶液を添加した後、Ag^+イオンとDPTAの濃度比は約3:17であり、調製したEC電解質溶液の10:1比よりもはるかに高かった(図2)。これらの結果から、DPTAはAg^+イオンと遊離し、複合種を形成しなかったことが示された。この結果は、DPTA存在下でもAg^+イオンの還元の臨界電位がシフトしないという図2(a)のCV結果を支持するものであった。

次に、Ag^+イオンを含まない電解液を用いて、DPTA単独の電気化学的活性を調べた(図2(b))。LiClのみを含む電解質溶液のCV(黒線)では、約-1.2 Vで電流が流れ始めた。この電流は、DMSOの吸湿性により、電解質溶液中に存在する少量の水が分解したためと考えられる。

また、DPTAを含む電解液(赤線)では、-1.7 Vで水の分解とは異なる還元電流が観測された。また、DPTAの反応部位を特定するために、EDTAとHEDTAのCV測定も行った。図S3に示す結果のCVでは、EDTAとHEDTAの還元と酸化は、DPTAとほぼ同じ電位で起こった。これらのEDTAおよびEDTA誘導体は3つまたは4つのカルボキシル基を有し、これらは段階的にプロトンを解離し、一価から四価のアニオンを形成する。1.7Vから観察される還元は、DPTAのこれらのカルボキシル基の還元に由来するはずであり、ラジカルアニオンの形成につながる。カルボキシル基は電気化学的に還元されてラジカルアニオンになることが知られている[55) 57)] さらに、DPTAを含む電解質では-1.4 Vに酸化ピークが現れた。このアノード電流は、DPTAのラジカルアニオンが中性状態に戻る酸化に起因しており、DPTAの中性アニオンとラジカルアニオンの間の可逆的な酸化還元挙動を示している。

図2(a)のCV測定において、DPTAの有無による透過率の違いの理由を検討するため、定電位印加時のQCM測定を行った。QCM法は、石英電極表面に析出したAgNPの質量を経時的に定量化することができる[58)]。CV測定に用いた作用電極を石英共振電極に置き換え(図S4)、-2.0Vの電位を120秒間印加した。対応する反応電荷とQCM発振周波数の変化を測定した。V=-2.0VではAg+イオンとDPTAの両方が還元されるため、DPTAを含むECデバイスの全反応電荷は、電位印加中に顕著に大きくなった(図3(a))。反応電荷の測定値は、DPTAありで235 mC/cm^2、DPTAなしで179 mC/cm^2であった。図3(b)は、全反応電荷量と蒸着質量の関係を示している。最小二乗法で求めた傾きから算出した1molあたりの質量は、それぞれ90g/mol(DPTAあり)、101g/mol(DPTAなし)であった。これらの値は、理論値である108g/mol(Agの原子量)よりも低い値であった。この違いは、計算された反応電荷が、電位印加直後に電気二重層を形成する非ファラデー電流を含んでいたために生じたと思われる。DPTAを含むEC装置での沈着質量は225μg/cm^2であり、DPTAなしで測定した185μg/cm^2を大幅に上回った。

end for returning to the positive direction) and –1.0 V (in the forward sweep to the positive direction) during the CV measurement. The transmission spectra were broad, and the wavelength dependence of the transmittance was not observed. Furthermore, as shown in Fig. 2(a), the minimum transmittance of the EC device containing DPTA was lower than that of the device without DPTA. These results suggested that DPTA influenced the coloration behavior of the EC device.

EDTA and DPTA are well-known metal-chelating agents that form complex species with metal cations. Therefore, potentiometric titration was performed to determine whether DPTA formed complex species with Ag^+ ions in the EC electrolyte solution. From our previous study, Ag^+ ions in the EC electrolyte solution form complex species with halide ions from the supporting electrolyte (Cl^- ions in this study). A 10 mL solution containing $AgCl_n^{(n-1)-}$ was prepared by dissolving 10 mM $AgNO_3$ and 50 mM LiCl in DMSO. The equilibrium potential was then measured while gradually adding a DMSO solution containing 25 mM DPTA to the $AgCl_n^{(n-1)-}$ solution. The equilibrium electrode potential for the Ag/Ag^+ redox reaction in the electrolyte solution was measured using an AgS wire as the indicating electrode and an Ag/Ag^+ reference electrode. The spontaneous potential change (Fig. S2) was monitored as the DPTA solution was gradually added to the electrolyte containing $AgCl_n^{(n-1)-}$. Before DPTA was added, the equilibrium potential was –0.65 V (vs. Ag/Ag^+). A total of 20 mL of the DPTA solution was incrementally introduced while measuring potential. As a result, the equilibrium electrode potential remained nearly stable around –0.64 V, even after adding 20 mL of DPTA solution. After adding 20 mL of DPTA solution, the concentration ratio between Ag^+ ions and DPTA was approximately 3:17, much higher than the 10:1 ratio in the prepared EC electrolyte solution (Fig. 2). These results indicate that DPTA remained free and did not form complex species with Ag^+ ions. This result supported the CV result in Fig. 2(a) that the critical potential of the reduction of Ag^+ ion was not shifted even in the presence of DPTA.

Next, the electrochemical activity of DPTA alone was investigated using an electrolyte solution without Ag^+ ions (Fig. 2(b)). In the CV of the electrolyte solution containing only LiCl (black line), a current began to flow at approximately –1.2 V. This current would be attributed to the decomposition of a small amount of water present in the electrolyte solution owing to the hygroscopic nature of DMSO. Besides, in the electrolyte solution containing DPTA (red line), a reduction current distinct from water decomposition was observed at –1.7 V. CV measurements were also conducted for EDTA and HEDTA to identify the reactive sites in DPTA. In the resulting CV shown in Fig. S3, the reduction and oxidation of EDTA and HEDTA occurred at nearly the same potential as DPTA. These EDTA and EDTA derivatives possess three or four carboxyl groups, which dissociate protons stepwise, forming mono- to tetravalent anions. The reduction observed from –1.7 V should be derived from the reduction of these carboxyl groups of DPTA, leading to the formation of radical anions. It is known that carboxyl groups can be electrochemically reduced to radical anions.[55)~57)] Additionally, in the electrolyte containing DPTA, an oxidation peak appeared at –1.4 V. This anodic current is attributed to the oxidation of the radical anion of DPTA back to its neutral state, indicating the reversible redox behavior of DPTA between its neutral and radical anion.

To investigate the reason for the difference in transmittance during CV measurement in Fig. 2(a) with or without DPTA, QCM measurement was conducted during constant potential application. The QCM method can quantify the mass of AgNPs deposited on the surface of a quartz electrode over time.[58)] The working electrode used in the CV measurement was replaced with a quartz resonator electrode (Fig. S4), and a potential of –2.0 V was applied for 120 s. The corresponding reacted charge and the change in QCM oscillation frequency were measured. Since both Ag^+ ions and DPTA are reduced at V = –2.0 V, the total reacted charge in the EC device containing DPTA was noticeably larger during the potential application (Fig. 3(a)). The measured reacted charges were 235 mC/cm^2 with DPTA and 179 mC/cm^2 without DPTA. Fig. 3(b) presents the relationship between the total reacted charge and the deposited mass. The mass per mol calculated from the slope obtained using the least squares method was 90 g/mol (with DPTA) and 101 g/mol (without DPTA), respectively. These values were lower than the theoretical value of 108 g/mol (atomic weight of Ag). This difference likely arose because the calculated reaction charge included a non-Faradaic current to form the electrical double layer immediately after potential application. The deposited mass was 225 μg/cm^2 in the EC device containing DPTA, significantly exceeding the 185 μg/cm^2 measured without DPTA. These results indicated that DPTA mediated electron transfer to

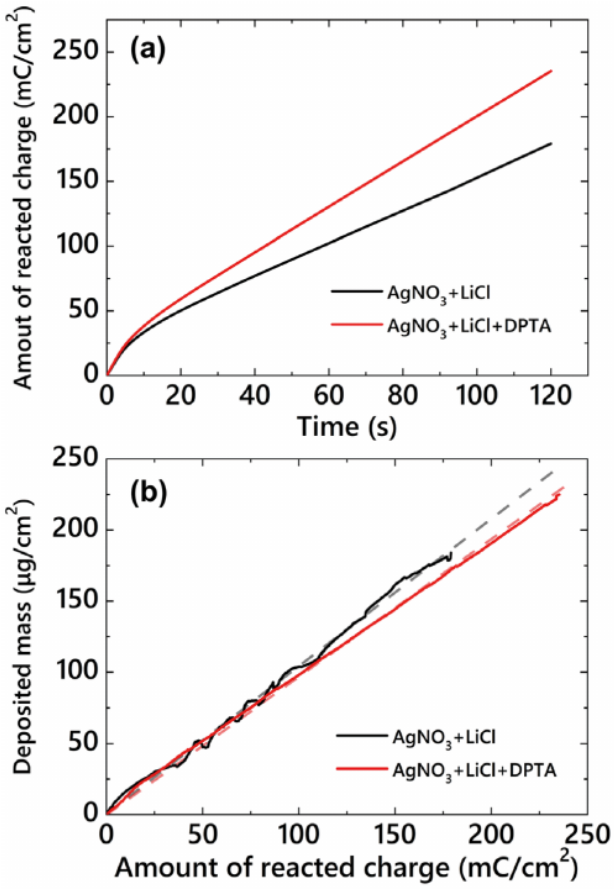

図3（a）3電極ECデバイスにV = −2.0 V（vs. Ag/Ag$^+$）を120秒間電位印加したときのQCMの反応電荷量と(b）蒸着質量。破線は各プロットについて最小二乗法による近似直線である。

これらの結果から、DPTAを介した電子移動によりAg$^+$イオンが還元され、AgNPsの電着が促進されることが示された。図2のCVによると

$$Ag^+ + e^- \rightarrow Ag^0 \qquad (at\ -1.2\ V\ vs.\ Ag/Ag^+)$$

$$[DPTA]^{n-} + e^- \rightarrow [DPTA]^{\bullet(n+1)-}\ (n: 0\text{-}4) \qquad (at\ -1.7\ V\ vs.\ Ag/Ag^+)$$

上記の式から

$$Ag^+ + [DPTA]^{\bullet(n+1)-} \rightarrow Ag^0 + [DPTA]^{n-}\ (n: 0\text{-}4)$$

上記の電気化学的媒介反応は、作用電極で起こるはずである。DPTAの還元剤は、自己消光と水酸化物イオンとの反応によって中性状態に戻るので、DPTAの有無によるEC電解質溶液間の1molあたりの計算質量の差は、DPTAのこの媒介反応に起因すると考えられる。

Ag蒸着ベースのECデバイスにおいて、印加電位を変化させながら、AgNPsの形態を電界放出型走査電子顕微鏡(FESEM)で調べた。

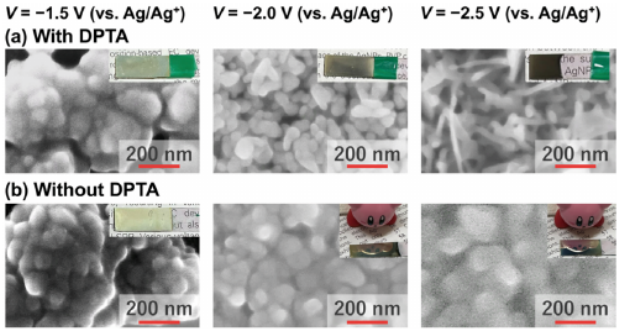

図4 −1.5V、−2.0V、−2.5Vを120秒間電位印加した後のECデバイス(a)と(b)のFE-SEM像。挿入図：電位印加後の作用電極上のAg層の写真。

図4は、3電極ECデバイスに−1.5 V、−2.0 V、−2.5 V(vs. Ag/Ag$^+$)を120秒間印加した後の作用電極のFE-SEM像である。DPTAを含むECデバイス(図4(a))では、−1.5Vを印加すると複雑な粒子間凝集が起こり、大きな塊が形成された。この成膜挙動は、図4(b)に示すように、DPTAを用いないECデバイスで観察されたものと同様であった。しかし、V = −2.0 Vでは、FE-SEM像に棒状のナノ粒子が現れ、長軸は約70~80 nm、平均アスペクト比は約2.7であった。さらに、−2.5 Vの場合、AgNPは針状に成長し、長軸は180~200 nm、アスペクト比は40以上であった。球状のAgNPは−1.5 Vで複雑に凝集したが、V = −2.0 Vや−2.5 Vのような高い電位をDPTAを含むECデバイスに印加すると、異方性AgNPが析出した。図S5は、−2.0Vと−2.5Vを印加したときのEDTAとHEDTAを用いたECデバイスのSEM像である。2.0V印加時、EDTA、HEDTAともにDPTAと異なり球状AgNPが析出した。2.5Vでは、EDTAとHEDTAにそれぞれ棒状と球状のAgNPが析出した。HEDTAについては、EDTA、DPTAと同じ電位で反応した。しかし、蒸着されたAgNPsの形態は影響を受けなかった。DPTA、EDTA、HEDTAの分子構造の違いが、蒸着されたAgNPの形態への影響を変化させた可能性がある。現在、AgNPsの分子構造と析出したモルフォロジーの関係について研究中である。

この沈着挙動の変化は、DPTAの減少に関係しているはずである。図2(b)のCVによると、DPTAの還元電位は−1.7 Vである。詳細な反応メカニズムは不明であるが、−1.7 Vより負の電位で生成したDPTAの還元剤は、析出したAgNPと相互作用し、ロッドや針のような異方性構造の形成を促進するようである。

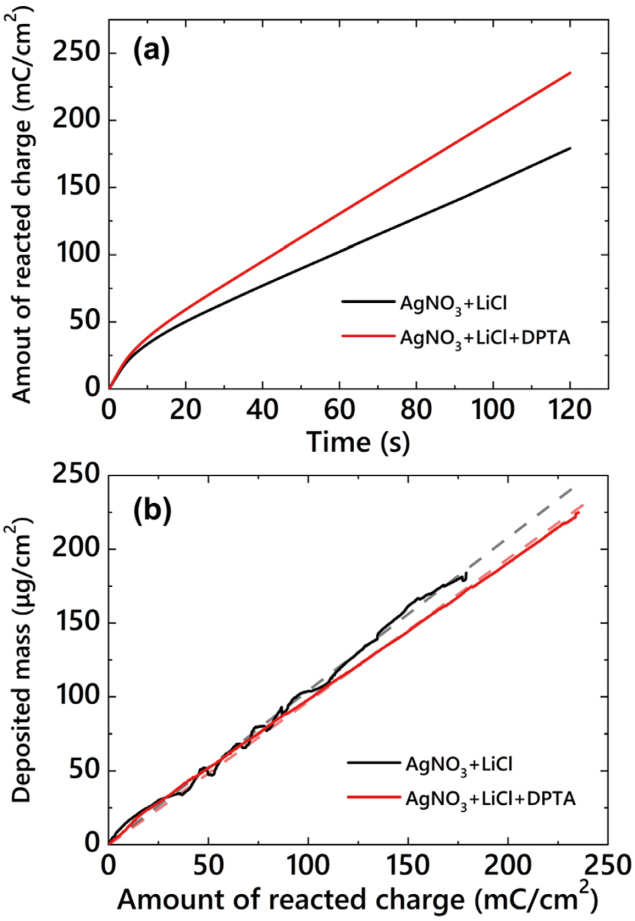

Fig. 3 (a) The amount of reacted charge and (b) deposited mass in QCM during potential application of $V = -2.0$ V (vs. Ag/Ag^+) for 120 s in the three-electrode EC device. Dashed lines are approximate straight lines using the least-squares method for each plot.

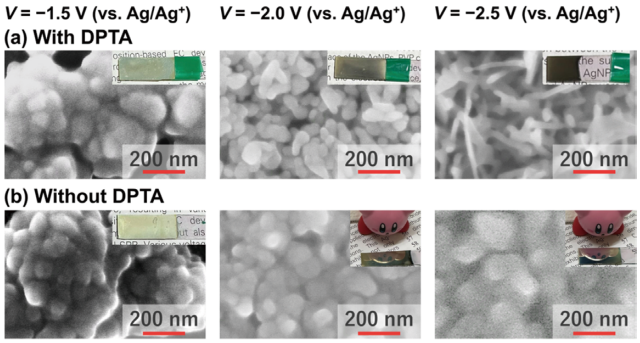

Fig. 4 FE-SEM images of the EC device (a) with and (b) without DPTA after potential application of –1.5 V, –2.0 V, and –2.5 V for 120 s. Inset: Photographs of the Ag layer on the working electrode after potential application.

reduce the Ag^+ ions, promoting the electrodeposition of AgNPs. According to the CV in Fig. 2,

$$Ag^+ + e^- \rightarrow Ag^0 \qquad (\text{at } -1.2 \text{ V vs. } Ag/Ag^+)$$

$$[DPTA]^{n-} + e^- \rightarrow [DPTA]^{\bullet(n+1)-} \text{ (n: 0-4)} \qquad (\text{at } -1.7 \text{ V vs. } Ag/Ag^+)$$

From the above equations,

$$Ag^+ + [DPTA]^{\bullet(n+1)-} \rightarrow Ag^0 + [DPTA]^{n-} \text{ (n: 0-4)}$$

The above electrochemical mediation reaction should occur at the working electrode. Since the reductant of DPTA returns to its neutral state through self-quenching and its reaction with hydroxide ions, the difference in the calculated mass per mol between the EC electrolyte solution with or without DPTA can be attributed to this mediation reaction of DPTA.

In the Ag deposition-based EC device, the morphology of AgNPs was investigated, varying the applied potential with a field-emission scanning electron microscope (FE-SEM). Fig. 4 shows FE-SEM images of the working electrode after applying –1.5 V, –2.0 V, and –2.5 V (vs. Ag/Ag^+) for 120 s in a three-electrode EC device. In the EC device containing DPTA (Fig. 4(a)), complex interparticle aggregation occurred upon applying –1.5 V, forming large clumps. This deposition behavior was similar to that observed in the EC device without DPTA, as shown in Fig. 4(b). However, at $V = -2.0$ V, rod-shaped nanoparticles appeared in the FE-SEM image, with long axes measuring approximately 70~80 nm and an average aspect ratio of about 2.7. Moreover, in the case of –2.5 V, the AgNPs grew into needle-like shapes, with long axes measuring 180~200 nm and aspect ratios of more than 40. While spherical AgNPs were complexly aggregated at –1.5 V, anisotropic AgNPs were deposited when a higher potential, such as $V = -2.0$ V or –2.5 V, was applied to the EC device containing DPTA. Fig. S5 shows SEM images of EC devices with EDTA and HEDTA when –2.0 V and –2.5 V were applied. When –2.0 V was applied, spherical AgNPs were deposited in the case of both EDTA and HEDTA, unlike DPTA. At –2.5 V, rod-shaped and spherical AgNPs were deposited for EDTA and HEDTA, respectively. Regarding the HEDTA, HEDTA reacted to the same potential as EDTA and DPTA. However, the morphology of deposited AgNPs was not affected. There is a possibility that differences in molecular structure between DPTA, EDTA, and HEDTA may have changed the effect on the morphology of deposited AgNPs. The relationship between the molecular structure and the deposited morphology of AgNPs is currently under study.

This change in deposition behavior should be related to the reduction of DPTA. According to the CV in Fig. 2(b), the reduction potential of DPTA is –1.7 V. While the detailed reaction mechanism remains unclear, the reductants of DPTA generated at a potential more

これらの結果は、DPTAを組み込んだECデバイスの動作電圧を変調することで、蒸着AgNPの異方性を制御できる可能性を示唆している。図4の挿入図は、DMSOとメタノールで洗浄した後のAgNP蒸着後の作用電極の写真である。1.5Vでは、DPTAを添加した電極も添加しない電極も、反射率なしで灰色の外観を示した。DPTAを含むECデバイスの場合(図4(a))、印加電位が高くなるにつれて、電極は徐々に濃い色調を示した。この暗色化は、電極上で粒子間成長する異方性ナノ粒子間の空間によって引き起こされる多重光散乱に起因すると考えられる。以前は、このような黒色発色のための多重散乱を達成するために、ITOナノ粒子を用いた作用電極表面への気孔率の導入が必要であった[35)43)]が、DPTAの存在下では、棒状や針状などの異方性AgNPの形成により、平坦なITO電極上でも黒色発色が達成された。図4(b)は、DPTA無添加のECデバイスに-1.5V、-2.0V、-2.5Vを印加した後のSEM像と電極写真である。すべてのケースで大きな粒子塊が形成され、灰色(V = -1.5 V)または反射状態(V = -2.0 Vおよび-2.5 V)となった。

蒸着したAgNPの形態を-2.0Vの定電位印加下でFE-SEMを用いて調べ、経時的な形態変化を調べた(図S6)。10秒と30秒では、電極表面全体に凝集した粒子が観察された(図S6(a)とS6(b))。電極の写真では、10秒後に灰色を呈し、表面被覆率が高くなるため、30秒後に鏡像状に変化した。60秒後、大きな塊の上に小さな凹凸が現れた。90秒と120秒の適用の可能性があり続けると、これらのアスペリティは徐々に棒状構造に発達した。このことは、棒状粒子はAg析出の初期段階では形成されず、むしろ一定量のAgNP析出後にAg塊上に出現したことを示している(図5)。この成長挙動の変化は、DPTA 還元剤の生成に関係しているはずである。電位印加直後、EC電解液中にDPTAの還元剤は存在しなかった。その結果、初期のAg析出挙動は、DPTAを用いないECデバイスで観察されたものと類似していた。

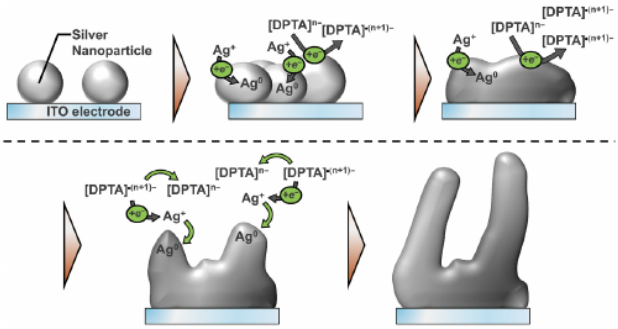

図5 DPTAを含むECデバイスにおけるAgNP成長の模式図。

しかし、DPTA還元剤の濃度が連続的な電位印加により徐々に上昇するにつれて、析出挙動は異方的な成長へとシフトした。これらの結果は、DPTA還元剤がAgNPsのロッド針状成長に重要な役割を果たしているという仮説を支持するものである。

2電極ECデバイスを作製するためには、Ag還元に伴う電荷を補償する反反応材料が必要であった。図S7は、Ag^+イオンを含む、以前に使用したEC電解質溶液に$CuCl_2$を添加した3電極ECデバイスのCV結果である。$CuCl_2$存在下でもAg析出の電気化学的応答は影響を受けなかった。$CuCl_2$を含まないECデバイスでは、透過率は約30%に回復しただけであったが、$CuCl_2$を含むデバイスでは、透過率はほぼ完全に100%に回復した。このように、$CuCl_2$を添加しても、DPTA存在下でもデバイス特性に悪影響はなかった。

$CuCl_2$を含む2電極ECデバイス(図S7、赤線と同じ)を、2つのITO電極を挟んで作製した(図S8)。ECデバイスの電気化学特性を評価した(図6)。Ag析出の臨界電圧は-2.3 Vと決定された。CuCl2が対極反応物質として機能するため、十分な量のAg析出が観察された。さらに、$CuCl_2$はこの2電極ECデバイスにおけるAgNPsの溶解を促進し、最初の透明状態に戻る可逆的な光学遷移を可能にした。前述したように、DPTAを還元することは、作用電極上で異方性AgNPを得るために不可欠である。2電極ECデバイスにおけるDPTAの反応電圧を決定するために、電圧掃引中の電極電位を図S9に示すセットアップを用いて測定した。図7は、作用電極(緑色の箇条書き)と対極(赤色の箇条書き)の電極電位の変化を示している。電圧掃引が0Vから開始されると、作用電極の電位は徐々に低下した。Ag^+イオンの還元は-2.3 Vで始まった。

negative than –1.7 V appear to interact with the deposited AgNPs, promoting the formation of rod- or needle-like anisotropic structures. These findings suggest that the anisotropy of deposited AgNPs can potentially be controlled by modulating the operating voltage of the EC device incorporating DPTA. The inset in Fig. 4 presents photographs of the working electrode after AgNP deposition, following washing with DMSO and methanol. At –1.5 V, both electrodes with and without DPTA exhibited a gray appearance without reflectivity. In the case of the DPTA-containing EC device (Fig. 4(a)), the electrode gradually exhibited a darker coloration as the applied potential increased. This darkening coloration would be attributed to multiple light scattering caused by the spaces between the interparticle growing anisotropic nanoparticles on the electrode. Previously, achieving such multiple scattering for black coloration required the introduction of porosity on the surface of the working electrode using ITO nanoparticles.[35)43)] However, in the presence of DPTA, black coloration was achieved even on a flat ITO electrode due to the formation of anisotropic AgNPs, such as rod- or needle-shaped. Fig. 4(b) presents SEM images and electrode photographs after applying –1.5 V, –2.0 V, and –2.5 V in the EC device without DPTA. Large particle clumps were formed in all cases, resulting in a grayish color (V = –1.5 V) or reflective state (V = –2.0 V and –2.5 V).

The morphology of deposited AgNPs was examined using FE-SEM under a constant potential application of –2.0 V to investigate morphological changes over time (Fig. S6). At 10 and 30 s, aggregated particles were observed across the entire electrode surface (Fig. S6(a) and S6(b)). Photographs of the electrode showed a grayish appearance at 10 s, which transitioned to a mirror-like state at 30 s due to increased surface coverage. At 60 s, small asperities appeared on top of the large clumps. With continued potential application at 90 and 120 s, these asperities gradually developed into rod-like structures. This indicates that rod-shaped particles did not form during the initial stage of Ag deposition but rather emerged on the Ag clumps after a certain amount of AgNP deposition (Fig. 5). This change in growth behavior should be related to the generation of DPTA reductants. Immediately after applying the potential, the reductants of DPTA were not present in the EC electrolyte solution. Consequently, the initial Ag deposition behavior resembled that observed in the EC device without DPTA. However, as the concentration of

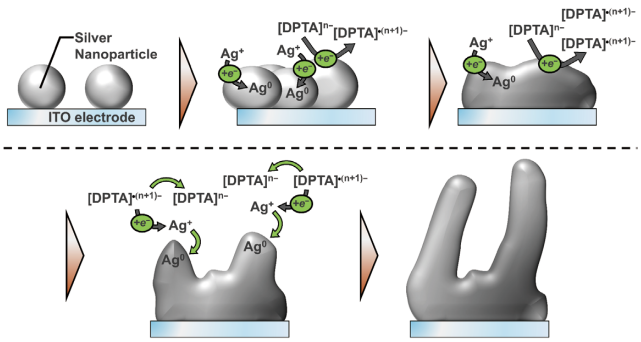

Fig. 5 Schematic diagram of the AgNP growth in the EC device containing DPTA.

DPTA reductants gradually increased due to continuous potential application, the deposition behavior shifted toward anisotropic growth. These results support the hypothesis that DPTA reductants play a key role in the rod- or needle-like growth of AgNPs.

A counter-reaction material was required to compensate for the charge associated with Ag reduction to fabricate the two-electrode EC devices. Fig. S7 presents the CV results of a three-electrode EC device with $CuCl_2$ added to the previously used EC electrolyte solution containing Ag^+ ions. The electrochemical response of the Ag deposition was not affected even in the presence of $CuCl_2$. In the EC device without $CuCl_2$, transmittance was only restored to approximately 30%, whereas in the device with $CuCl_2$, transmittance was almost fully recovered to 100%. Thus, adding $CuCl_2$ did not negatively impact the device properties, even in the presence of DPTA.

The two-electrode EC device containing $CuCl_2$ (same as in Fig. S7, red line) was fabricated by sandwiching two ITO electrodes (Fig. S8). The electrochemical properties of the EC device were evaluated (Fig. 6). The critical voltage for Ag deposition was determined to be –2.3 V. A sufficient amount of Ag deposition was observed, as CuCl2 functioned as the counter-electrode reactant. Additionally, $CuCl_2$ facilitated the dissolution of AgNPs in this two-electrode EC device, enabling a reversible optical transition back to the initial transparent state. As mentioned earlier, reducing DPTA is essential for obtaining anisotropic AgNPs on the working electrode. To determine the reaction voltage of DPTA in the two-electrode EC device, the electrode potentials during the voltage sweep were measured using the setup shown in Fig. S9. Fig. 7 indicates the changes in electrode potential for the working electrode (green bullets) and the counter electrode (red bullets). As the voltage sweep commenced from 0 V, the potential of

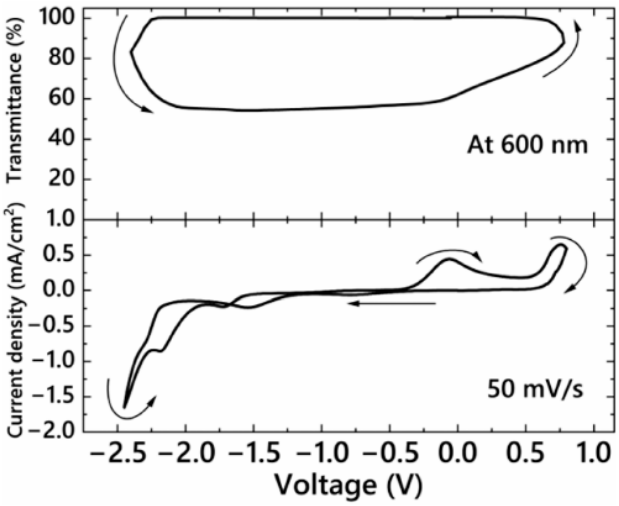

図6 $AgNO_3$, LiCl, $CuCl_2$, DPTAを含む2電極ECデバイスの600nmにおける透過率（上）とCV（下）の変化。

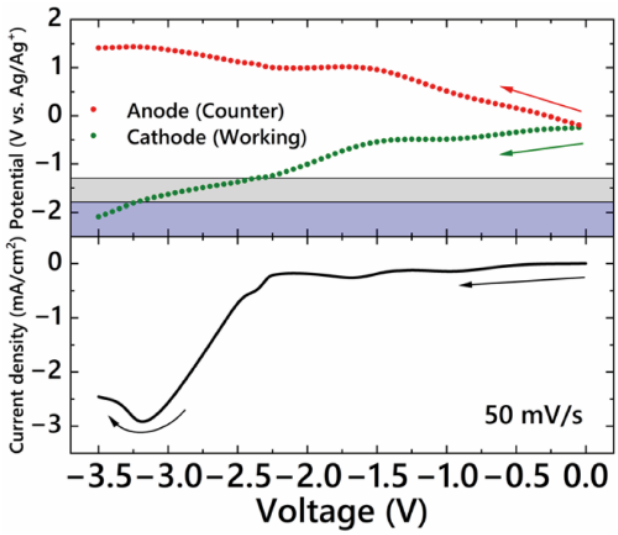

Fig. 7 2電極ECデバイスの電圧掃引（上）およびボルタンモグラム（下）におけるカソード（緑色の箇条書き）アノード（赤色の箇条書き）の電極電位の変化。灰色の領域はAg、青色の領域はDPTAを低減できる電位範囲をそれぞれ示している（図2参照）。

さらに電圧掃引を行うと、印加電圧-3.2 Vで作用電極の電位は-1.7 V（vs. Ag/Ag^+）に達した。図2(b)に示すように、DPTAの還元が始まる電位は-1.7 V（vs. Ag/Ag^+）であるため、ECデバイスが-2.3～-3.2 Vの電圧で動作すると、Ag^+イオンのみが還元されることになる。さらに、-3.2V以上の負電圧を印加すると、Ag^+イオンとDPTA還元が同時に起こり、

図4(a)に示すように異方性AgNPが形成される。

最後に、DPTAを用いた場合と用いない場合の2電極ECデバイスの光学特性を調べた。DPTAを低減できる-3.5Vの定電圧をECデバイスに50秒間印加した。電圧印加時の光学測定結果を図8に示す。DPTAの有無にかかわらず、この電圧条件下では透過率はほぼ0%に減少した（図8(a)）。しかし、DPTAを含むECデバイスでは、反射率が20%以下に抑制され（図8(b)）、光学状態が黒くなった（図8(c)）。この20%には数個のITO電極の反射率が含まれており、その値は前回の研究の黒色状態とほぼ同じであった[35]。この黒色は図4で観察された光学状態に対応しており、2電極ECデバイスではDPTAが減少していることが示唆された。一方、DPTAを用いないデバイスは、平坦なAg層が形成されているため、鏡面的な状態（図8(d)）を示し、高い反射率は100%（図8(b)）に近づいた。DPTAの影響は、電圧印加直後から明らかになった。10秒後、DPTAを含むECデバイスは灰色に見えるが、DPTAを含まないデバイスは弱い反射状態を示した。電圧印加を続けると、DPTAを含むECデバイスの光学状態は明瞭な黒に遷移し、その結果、t = 50秒では深い黒色になった。一方、DPTAを用いないEC装置では、50秒の時点で明らかなミラー状態が得られた。ITOナノ粒子で修飾した従来の多孔質ITO電極では黒色着色に約20秒かかったのに対し、DPTAを用いたECデバイスでは50秒かかった。これは、ITOナノ粒子修飾ITO電極を使用した場合、AgNPは多孔質構造の表面にのみ析出するが、AgNP自体はDPTAを使用してECデバイスで多孔質構造を形成する必要があるためである。しかし、ECデバイスの色付けには50秒程度であり、複雑な電極作製工程を経ずに適用を最適化することで、応答特性を向上させることができる。

potential and concentration of components of EC electrolyte solution. Besides, it is possible to maintain this black color by the application of a pulse voltage for Ag reduction, preventing the thorough dissolution of AgNPs. Although the black color in conventional Ag deposition-based EC devices was provided by preparing the electrode surface porous with ITO nanoparticles, transmittance was reduced owing to light scattering by ITO nanoparticles in the transparent state.[35] However, DPTA achieved black color with high optical contrast

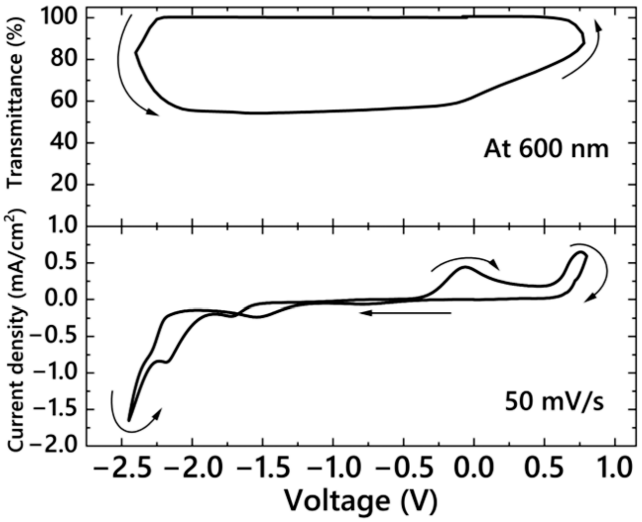

Fig. 6 Change in transmittance at 600 nm (top) and CV (bottom) of the two-electrode EC device containing $AgNO_3$, LiCl, $CuCl_2$, and DPTA.

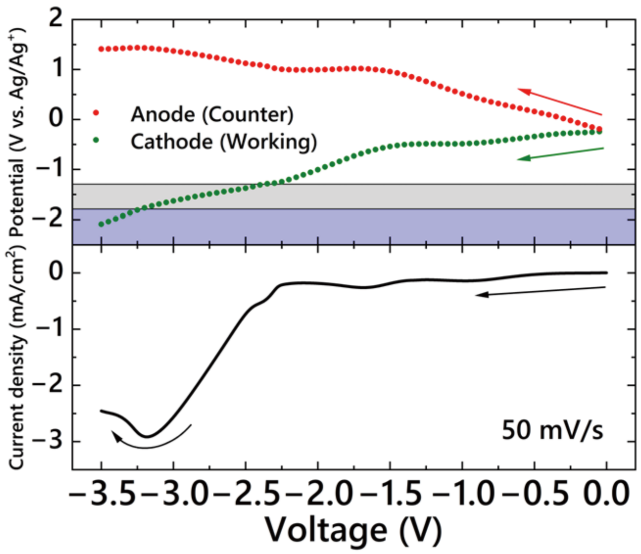

Fig. 7 Changes in electrode potential of the cathode (green bullets) anodes (red bullets) during voltage sweep (top) and voltammogram (bottom) of two-electrode EC device. The gray and blue areas indicate the potential range in which Ag and DPTA can be reduced, respectively (refer to Fig. 2).

the working electrode gradually decreased. The reduction of Ag^+ ions began at –2.3 V. With further voltage sweeping, the potential of the working electrode reached –1.7 V (vs. Ag/Ag^+) at an applied voltage of –3.2 V. Since –1.7 V (vs. Ag/Ag^+) is the potential at which DPTA reduction begins, as shown in Fig. 2(b), it follows that when the EC device operates at voltages between –2.3 and –3.2 V, only Ag^+ ions are reduced. Furthermore, when a voltage more negative than –3.2 V is applied, Ag^+ ions and DPTA reduction occur simultaneously, leading to anisotropic AgNPs forming, as observed in Fig. 4(a).

Finally, the optical properties of two-electrode EC devices with and without DPTA were investigated. A constant voltage of –3.5 V, at which DPTA can be reduced, was applied to the EC devices for 50 s. The results of the optical measurements during voltage application are shown in Fig. 8. Regardless of the presence or absence of DPTA, the transmittance decreased to nearly 0% under this voltage condition (Fig. 8(a)). However, in the EC device containing DPTA, the reflectance was suppressed to below 20% (Fig. 8(b)), resulting in a black optical state (Fig. 8(c)). This 20% included the reflectance of a couple of ITO electrodes, and the value was almost the same compared to the black state in our previous study.[35] This black coloration corresponded to the optical state observed in Fig. 4, suggesting that DPTA was reduced in the two-electrode EC device. In contrast, the device without DPTA exhibited a mirror-like state (Fig. 8(d)) with high reflectivity approaching 100% (Fig. 8(b)) due to the formation of a flat Ag layer. The influence of DPTA became apparent immediately after voltage application. At 10 s, the EC device containing DPTA appeared gray, whereas the device without DPTA exhibited a weak reflective state. With continued voltage application, the optical state of the EC device containing DPTA transitioned to a distinct black, and the resulting optical state was a deep black color at t = 50 s. Contrarily, the EC device without DPTA provided an apparent mirror state at the time of 50 s. Black coloration with conventional porous ITO electrode modified with ITO nanoparticles took about 20 s, whereas 50 s was taken in the EC device with DPTA. This is because AgNPs are deposited only on the surface of the porous structure when an ITO nanoparticle-modified ITO electrode is used, though AgNPs themselves must form the porous structure in the EC device using DPTA. However, 50 s sufficient for coloration of EC devices, and the response property can be improved by optimizing the applied potential and concentration of components of EC electrolyte solution. Besides, it is possible to maintain this black color by the application of a pulse voltage for Ag reduction, preventing the thorough dissolution of AgNPs. Although the black color in conventional Ag deposition-based EC devices was provided by preparing the electrode surface porous with ITO nanoparticles, transmittance was reduced owing to light scattering by ITO nanoparticles in the transparent state.[35] However, DPTA achieved black color with high optical contrast

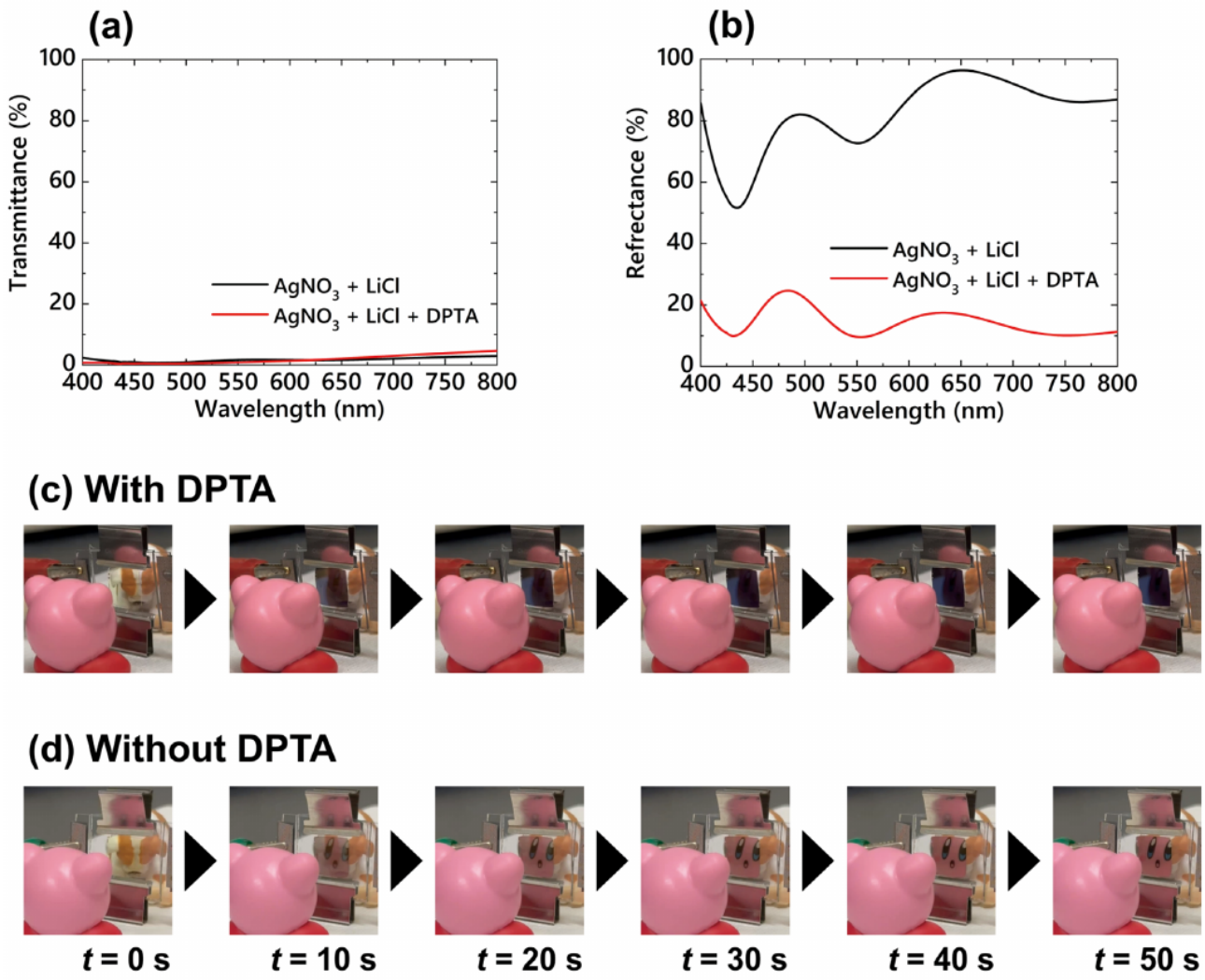

図8（a）V = -3.5 V、50秒の電圧印加後の2電極ECデバイスの透過スペクトルと(b）反射スペクトル。写真: 写真:ECデバイスの光学状態の変化(c)DPTAあり、(d)DPTAなし。

図6のCV結果から、$CuCl_2$を用いたECデバイスは、DPTAの有無にかかわらず十分なサイクル安定性を示した。図S10は、-2.7Vを50秒間印加したときのECデバイスの写真である。DPTAは-2.7 Vでは反応しないため、DPTAを用いたECデバイス(図S10(a))とDPTAを用いないECデバイス(図S10(b))は、鏡面反射を伴う同様のミラー状態を示した。したがって、デバイスの動作電圧を操作することで、透明状態からミラー状態、フラット電極上の黒状態への任意スイッチングを実現した。

4むすび

本研究では、EDTAの誘導体であるDPTAを導入し、Ag蒸着ベースのECデバイスにおけるAgNPsのモルフォロジーを制御することを目的とした。DPTAはAgNPのキャッピング剤として機能し、異方性モルフォロジーの形成を促進することが期待された。ECデバイスの電気化学的特性、形態学的特性、光学的特性に及ぼすPVP導入の影響について検討した。

電位差滴定により、DPTAはEC電解質中でAg^+イオンと複合種を形成しないことが明らかになった。しかし、DPTAは電気化学的活性を示し、その酸化還元反応は可逆的であることがわかった。一旦還元されると、DPTAのラジカルアニオンがAg^+イオンへの電子移動を媒介し、析出を促進し、ナノ粒子の形態を変化させる。2.0Vまたは-2.5Vの電位を印加すると、棒状および針状の異方性ナノ粒子が作用電極上に析出した。この異方性形態への移行は、DPTA還元剤の生成に関連していると考えられる。これらの異方性構造は粒子間空間を作り出し、多孔質基板を持つ電極を使用することなく、多重光散乱と黒色化をもたらした。

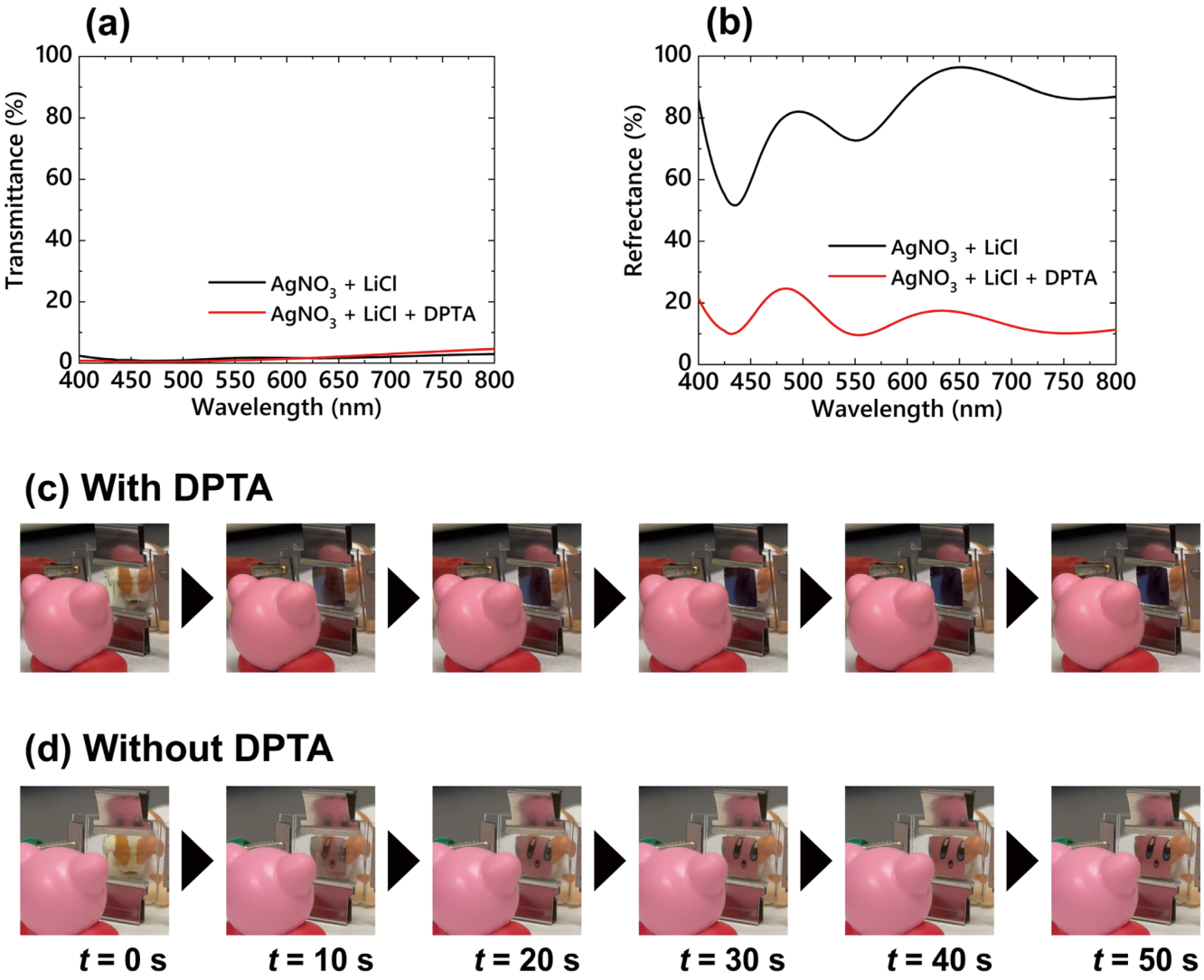

Fig. 8 (a) Transmission and (b) reflection spectra of the two-electrode EC device after the voltage application of $V = -3.5$ V for 50 s. Photographs: Change in the optical states of the EC device (c) with and (d) without DPTA.

without a complicated electrode preparation process. From the CV result in Fig. 6, the EC device with $CuCl_2$ had enough cyclic stability regardless of the presence of DPTA. Fig. S10 shows photographs of the EC devices when –2.7 V is applied for 50s. Since DPTA cannot react at –2.7 V, both EC devices with DPTA (Fig. S10(a)) and without DPTA (Fig. S10(b)) exhibited a similar mirror state with specular reflection. Therefore, arbitrarily switching from the transparent state to the mirror and the black state on the flat electrode was achieved by manipulating the device operation voltage.

4. Conclusion

In this study, DPTA, a derivative of EDTA, was introduced to control the morphology of AgNPs in an Ag deposition-based EC device. DPTA was expected to function as a capping agent for AgNPs, facilitating the formation of anisotropic morphologies. The effects of introducing PVP on the electrochemical, morphological, and optical properties of the EC device were investigated.

Potentiometric titrations revealed that DPTA did not form complex species with Ag^+ ions in the EC electrolyte. However, DPTA exhibited electrochemical activity, and its redox reaction was found to be reversible. Once reduced, the radical anion of DPTA mediated electron transfer to Ag^+ ions, enhancing deposition and altering nanoparticle morphology. When a potential of –2.0 V or –2.5 V was applied, rod- and needle-like anisotropic nanoparticles were deposited on the working electrode. This transition toward anisotropic morphologies is likely associated with generating DPTA reductants. These anisotropic structures created interparticle spaces, leading to multiple light scattering and black coloration without using an electrode with a porous substrate.

また、DPTAを印加したEDデバイスは、DPTAが反応しない電圧を印加するとミラー状態を示した。このように、ECデバイスの動作電圧を制御することで、ミラーと黒の状態を任意に切り替えることができた。

本研究では、Ag析出ベースのECシステムにEDTA誘導体を導入することで、ECデバイスにおけるAgNPsの電着モルフォロジーを制御する新しい方法を実証した。全体として、本研究は、DPTA変調が、電気化学系においてもAgNPsの成長挙動を効果的に制御できることを強調している。この理解のさらなる進歩により、高い色純度を持つ新しい色の開発が可能になる可能性がある。電気化学的に生成された金属ナノ粒子の形態を精密に制御することは、Ag LSPR ベースのエレクトロクロミズムに加え、貴金属触媒やプラズモニック粒子ベースのバイオセンサーなど、幅広い分野に貢献することが期待される。

本研究は、日本学術振興会科研費(15H03880、17H06377、19J21962、22H02154)、科学技術振興機構(A-STEP:AS2915036S、SPRING:JPMJSP2109)、笹川科学研究費補助金(2023-2022)の助成を受けた。

References

1) Argun, A. A.; Aubert, P. H.; Thompson, B. C.; Schwendeman, I.; Gaupp, C. L.; Hwang, J.; Pinto, N. J.; Tanner, D. B.; MacDiarmid, A. G.; Reynolds, J. R.: "Multicolored Electrochromisin in Polymer Structures and Devices", Chemistry of Materials 16, 23, pp.4401-4412 (Nov. 16, 2004)
2) Watanabe, A.; Mori, K.; Iwasaki, Y.; Nakamura, Y.; Niizuma, S.: "Electrochromism of Polyaniline Film Prepared by Electrochemical Polymerization", Macromolecules 20, , pp.1793-1796 (1987)
3) Higuchi, M.; Fujii, Y.: "Designed, Flexible Electrochromic Display Device with Fe(II)-Based Metallo-Supramolecular Polymer Using Mechanically Etched ITO Film", Journal of Photopolymer Science and Technology 34, , pp.175-180 (Nov. 2021)
4) Mjejri, I.; Doherty, C. M.; Rubio-Martinez, M.; Drisko, G. L.; Rougier, A.: "Double-Sided Electrochromic Device Based on Metal-Organic Frameworks", ACS Appl Mater Interfaces 9, 46, pp.39930-39934 (Nov. 22, 2017)
5) Urano, H.; Sunohara, S.; Ohtomo, H.; Kobayashi, N.: "Electrochemical and Spectroscopic Characteristics of Dimethyl Terephthalate", J Mater Chem 14, 15, pp.2366-2368 (Aug. 7, 2004)
6) Ribeiro, A. S.; Nogueira, V. C.; Faria dos Santos Filho, P.; De Paoli, M. A.: "Electrochromic Properties of Poly{3-[12-(Methoxyphenoxy)Dodecyl]Thiophene}", Electrochim Acta 49, 14, pp.2237-2242 (June 15, 2004)
7) Hsiao, S. H.; Chen, Y. Z.: "Electrosynthesis of Redox-Active and Electrochromic Polymer Films from Triphenylamine-Cored Star-Shaped Molecules End-Capped with Arylamine Groups", Eur Polym J 99, , pp.422-436 (Feb. 1, 2018)
8) Liang, Z.; Nakamura, K.; Kobayashi, N.: "A Multicolor Electrochromic Device Having Hybrid Capacitor Architecture with a Porous Carbon Electrode", Solar Energy Materials and Solar Cells 200, (Sep. 15, 2019)
9) Mortimer, R. J.: "Organic Electrochromic Materials", Electrochim Acta 44, 18, pp.2971-2981 (May 1, 1999)
10) Maciossek, A.; Lochel, B.; Schulze, S.; Noetzel, J.; Quenzer, H.; Wagner, B.; Eng, M.; Konig, M.; Huber, H.; KUnig, M.; of ACTUATOR, P.; Borgmann, H.; Lenz, K.; Bauer, G.; L Noltent, P. H.; Kremers, M.; Griessen, R.: "Optical Switching of Y-Hydride Thin Film Electrodes A Remarkable Elecfrochromic Phenomenon", Microelectron. Eng 143, 10, pp.455 (1996)
11) Richardson, T. J.; Slack, J. L.; Farangis, B.; Rubin, M. D.: "Mixed Metal Films with Switchable Optical Properties", Appl Phys Lett 80, 8, pp.1349-1351 (Feb. 25, 2002)
12) Tajima, K.; Yamada, Y.; Okada, M.; Yoshimura, K.: "Surface Coating of Electrochromic Switchable Mirror Glass Based on Mg-Ni Thin Film for High Durability in the Environment", Applied Physics Express 3, 4 (Apr. 2010)
13) Kondo, Y.; Tanabe, H.; Kudo, H.; Nakano, K.; Otake, T.: "Electrochromic Type E-Paper Using Poly(1H-Thieno[3, 4-d] Imidazol-2(3H)-One) Derivatives by a Novel Printing Fabrication Process", Materials 4, 12, pp.2171-2182 (2011)
14) Kobayashi, N.; Miura, S.; Nishimura, M.; Urano, H.: "Organic Electrochromism for a New Color Electronic Paper", Solar Energy Materials and Solar Cells 92, 2, pp.136-139 (Feb. 2008)
15) Corr, D.; Bach, U.; Fay, D.; Kinsella, M.; McAtamney, C.; O'Reilly, F.; Rao, S. N.; Stobie, N.: "Coloured Electrochromic: "Paper-Quality" Displays Based on Modified Mesoporous Electrodes", Solid State Ion 165, 1-4, pp.315-321 (Dec. 2003)
16) Granqvist, C. G.: "Electrochromics for Smart Windows: Oxide-Based Thin Films and Devices", Thin Solid Films 564, , pp.1-38 (Aug. 1, 2014)
17) Niklasson, G. A.; Granqvist, C. G.: "Electrochromics for Smart Windows: Thin Films of Tungsten Oxide and Nickel Oxide and Devices Based on These", J Mater Chem 17, 2, pp.127-156 (2007)
18) Gillaspie, D. T.; Tenent, R. C.; Dillon, A. C.: "Metal-Oxide Films for Electrochromic Applications: Present Technology and Future Directions", J Mater Chem 20, 43, pp.9585-9592 (Nov. 21, 2010)
19) Rosseinsky, D. R.; Mortimer, R. J.: "Electrochromic Systems and the Prospects for Devices", Advanced Materials 13, 11, pp.783-793 (June 5, 2001)
20) Granqvist, C. G.: "Electrochromic Tungsten Oxide Films: Review of Progress 1993-1998", Solar Energy Materials and Solar Cells 60, 3, pp.201-262 (2000)
21) Richardson, T. J.; Slack, J. L.; Armitage, R. D.; Kostecki, R.; Farangis, B.; Rubin, M. D.: "Switchable Mirrors Based on Nickel-Magnesium Films", Appl Phys Lett 78, 20, pp.3047-3049 (May 14, 2001)
22) Bach, U.; Corr, D.; Lupo, D.; Pichot, F.; Ryan, M.: "Nanomaterials-Based Electrochromics for Paper-Quality Displays", Advanced Materials 14, 11, pp.845-848 (June 2002)
23) Venugopal, R.; Dinakaran, A.; Nair, M. C.; Balachandran, A. C.; Madhavan, N. D.; Deb, B.: " Electrochromic Properties of MnO 2 /WO 3 Bilayered Electrodes for Enhanced Charge Storage and Superior Stability: ", RSC Applied Interfaces 1, 6, pp.1382-1394 (2024)
24) Reyes-Gil, K. R.; Stephens, Z. D.; Stavila, V.; Robinson, D. B.: "Composite WO3/TiO2 Nanostructures for High Electrochromic Activity", ACS Appl Mater Interfaces 7, 4, pp.2202-2213 (Feb. 4, 2015)
25) Kim, K. H.; Kahuku, M.; Abe, Y.; Kawamura, M.; Kiba, T.: "Improved Electrochromic Performance in Nickel Oxide Thin Film by Zn Doping", Int J Electrochem Sci 15, , pp.4065-4071 (2020)
26) Xia, X. H.; Tu, J. P.; Zhang, J.; Wang, X. L.; Zhang, W. K.; Huang, H.: "Electrochromic Properties of Porous NiO Thin Films Prepared by a Chemical Bath Deposition", Solar Energy Materials and Solar Cells 92, 6, pp.628-633 (June 2008)
27) Lee, S. H.; Deshpande, R.; Parilla, P. A.; Jones, K. M.; To, B.; Mahan, A. H.; Dillon, A. C.: "Crystalline WO3 Nanoparticles for Highly Improved Electrochromic Applications", Advanced Materials 18, 6, pp.763-766 (Mar. 17, 2006)
28) Baeck, S. H.; Choi, K. S.; Jaramillo, T. F.; Stucky, G. D.; McFarland, E. W.: "Enhancement of Photocatalytic and Electrochromic Properties of Electrochemically Fabricated Mesoporous WO3 Thin Films", Advanced Materials 15, 15, pp.1269-1273 (Aug. 5, 2003)
29) Jeong, K. R.; Lee, I.; Park, J. Y.; Choi, C. S.; Cho, S. H.; Lee, J. L.:

Also, the ED device with DPTA exhibited a mirror state when a voltage to which DPTA did not react was applied. Thus, arbitrarily switching the mirror and the black state was achieved by controlling the EC device operation voltage.

This study demonstrated a novel method for controlling the electrodeposited morphology of AgNPs in an EC device by introducing an EDTA derivative in an Ag deposition-based EC system. Overall, this work highlights that DPTA modulation can effectively control the growth behavior of AgNPs, even in an electrochemical system. Further advancements in this understanding could enable the development of new colors with high color purity. The precise control of the morphology of electrochemically generated metal nanoparticles is expected to contribute to a wide range of fields, including precious metal catalysts and plasmonic particle-based biosensors, in addition to Ag LSPR-based electrochromism.

This study was supported by JSPS KAKENHI (15H03880, 17H06377, 19J21962, and 22H02154), Japan Science and Technology Agency (A-STEP: AS2915036S, SPRING: JPMJSP2109), and Sasakawa Scientific Research Grant (2023-2022).

References

1) Argun, A. A.; Aubert, P. H.; Thompson, B. C.; Schwendeman, I.; Gaupp, C. L.; Hwang, J.; Pinto, N. J.; Tanner, D. B.; MacDiarmid, A. G.; Reynolds, J. R.: "Multicolored Electrochromisin in Polymers: Structures and Devices", Chemistry of Materials 16, 23, pp.4401-4412 (Nov. 16, 2004)
2) Watanabe, A.; Mori, K.; Iwasaki, Y.; Nakamura, Y.; Niizuma, S.: "Electrochromism of Polyaniline Film Prepared by Electrochemical Polymerization", Macromolecules 20, , pp.1793-1796 (1987)
3) Higuchi, M.; Fujii, Y.: "Designed, Flexible Electrochromic Display Device with Fe(II)-Based Metallo-Supramolecular Polymer Using Mechanically Etched ITO Film", Journal of Photopolymer Science and Technology 34, , pp.175-180 (Nov. 2021)
4) Mjejri, I.; Doherty, C. M.; Rubio-Martinez, M.; Drisko, G. L.; Rougier, A.: "Double-Sided Electrochromic Device Based on Metal-Organic Frameworks", ACS Appl Mater Interfaces 9, 46, pp.39930-39934 (Nov. 22, 2017)
5) Urano, H.; Sunohara, S.; Ohtomo, H.; Kobayashi, N.: "Electrochemical and Spectroscopic Characteristics of Dimethyl Terephthalate", J Mater Chem 14, 15, pp.2366-2368 (Aug. 7, 2004)
6) Ribeiro, A. S.; Nogueira, V. C.; Faria dos Santos Filho, P.; De Paoli, M. A.: "Electrochromic Properties of Poly{3-[12-(p-Methoxyphenoxy)Dodecyl]Thiophene}", Electrochim Acta 49, 14, pp.2237-2242 (June 15, 2004)
7) Hsiao, S. H.; Chen, Y. Z.: "Electrosynthesis of Redox-Active and Electrochromic Polymer Films from Triphenylamine-Cored Star-Shaped Molecules End-Capped with Arylamine Groups", Eur Polym J 99, , pp.422-436 (Feb. 1, 2018)
8) Liang, Z.; Nakamura, K.; Kobayashi, N.: "A Multicolor Electrochromic Device Having Hybrid Capacitor Architecture with a Porous Carbon Electrode", Solar Energy Materials and Solar Cells 200, (Sep. 15, 2019)
9) Mortimer, R. J.: "Organic Electrochromic Materials", Electrochim Acta 44, 18, pp.2971-2981 (May 1, 1999)
10) Maciossek, A.; Lochel, B.; Schulze, S.; Noetzel, J.; Quenzer, H.; Wagner, B.; Eng, M.; Konig, M.; Huber, H.; KUnig, M.; of ACTUATOR, P.; Borgmann, H.; Lenz, K.; Bauer, G.; L Noltent, P. H.; Kremers, M.; Griessen, R.: "Optical Switching of Y-Hydride Thin Film Electrodes A Remarkable Elecfrochromic Phenomenon", Microelectron. Eng 143, 10, pp.455 (1996)
11) Richardson, T. J.; Slack, J. L.; Farangis, B.; Rubin, M. D.: "Mixed Metal Films with Switchable Optical Properties", Appl Phys Lett 80, 8, pp.1349-1351 (Feb. 25, 2002)
12) Tajima, K.; Yamada, Y.; Okada, M.; Yoshimura, K.: "Surface Coating of Electrochromic Switchable Mirror Glass Based on Mg-Ni Thin Film for High Durability in the Environment", Applied Physics Express 3, 4 (Apr. 2010)
13) Kondo, Y.; Tanabe, H.; Kudo, H.; Nakano, K.; Otake, T.: "Electrochromic Type E-Paper Using Poly(1H-Thieno[3, 4-d] Imidazol-2(3H)-One) Derivatives by a Novel Printing Fabrication Process", Materials 4, 12, pp.2171-2182 (2011)
14) Kobayashi, N.; Miura, S.; Nishimura, M.; Urano, H.: "Organic Electrochromism for a New Color Electronic Paper", Solar Energy Materials and Solar Cells 92, 2, pp.136-139 (Feb. 2008)
15) Corr, D.; Bach, U.; Fay, D.; Kinsella, M.; McAtamney, C.; O'Reilly, F.; Rao, S. N.; Stobie, N.: "Coloured Electrochromic: "Paper-Quality" Displays Based on Modified Mesoporous Electrodes", Solid State Ion 165, 1-4, pp.315-321 (Dec. 2003)
16) Granqvist, C. G.: "Electrochromics for Smart Windows: Oxide-Based Thin Films and Devices", Thin Solid Films 564, , pp.1-38 (Aug. 1, 2014)
17) Niklasson, G. A.; Granqvist, C. G.: "Electrochromics for Smart Windows: Thin Films of Tungsten Oxide and Nickel Oxide and Devices Based on These", J Mater Chem 17, 2, pp.127-156 (2007)
18) Gillaspie, D. T.; Tenent, R. C.; Dillon, A. C.: "Metal-Oxide Films for Electrochromic Applications: Present Technology and Future Directions", J Mater Chem 20, 43, pp.9585-9592 (Nov. 21, 2010)
19) Rosseinsky, D. R.; Mortimer, R. J.: "Electrochromic Systems and the Prospects for Devices", Advanced Materials 13, 11, pp.783-793 (June 5, 2001)
20) Granqvist, C. G.: "Electrochromic Tungsten Oxide Films: Review of Progress 1993-1998", Solar Energy Materials and Solar Cells 60, 3, pp.201-262 (2000)
21) Richardson, T. J.; Slack, J. L.; Armitage, R. D.; Kostecki, R.; Farangis, B.; Rubin, M. D.: "Switchable Mirrors Based on Nickel-Magnesium Films", Appl Phys Lett 78, 20, pp.3047-3049 (May 14, 2001)
22) Bach, U.; Corr, D.; Lupo, D.; Pichot, F.; Ryan, M.: "Nanomaterials-Based Electrochromics for Paper-Quality Displays", Advanced Materials 14, 11, pp.845-848 (June 2002)
23) Venugopal, R.; Dinakaran, A.; Nair, M. C.; Balachandran, A. C.; Madhavan, N. D.; Deb, B.: " Electrochromic Properties of MnO 2 /WO 3 Bilayered Electrodes for Enhanced Charge Storage and Superior Stability: ", RSC Applied Interfaces 1, 6, pp.1382-1394 (2024)
24) Reyes-Gil, K. R.; Stephens, Z. D.; Stavila, V.; Robinson, D. B.: "Composite WO3/TiO2 Nanostructures for High Electrochromic Activity", ACS Appl Mater Interfaces 7, 4, pp.2202-2213 (Feb. 4, 2015)
25) Kim, K. H.; Kahuku, M.; Abe, Y.; Kawamura, M.; Kiba, T.: "Improved Electrochromic Performance in Nickel Oxide Thin Film by Zn Doping", Int J Electrochem Sci 15, , pp.4065-4071 (2020)
26) Xia, X. H.; Tu, J. P.; Zhang, J.; Wang, X. L.; Zhang, W. K.; Huang, H.: "Electrochromic Properties of Porous NiO Thin Films Prepared by a Chemical Bath Deposition", Solar Energy Materials and Solar Cells 92, 6, pp.628-633 (June 2008)
27) Lee, S. H.; Deshpande, R.; Parilla, P. A.; Jones, K. M.; To, B.; Mahan, A. H.; Dillon, A. C.: "Crystalline WO3 Nanoparticles for Highly Improved Electrochromic Applications", Advanced Materials 18, 6, pp.763-766 (Mar. 17, 2006)
28) Baeck, S. H.; Choi, K. S.; Jaramillo, T. F.; Stucky, G. D.; McFarland, E. W.: "Enhancement of Photocatalytic and Electrochromic Properties of Electrochemically Fabricated Mesoporous WO3 Thin Films", Advanced Materials 15, 15, pp.1269-1273 (Aug. 5, 2003)
29) Jeong, K. R.; Lee, I.; Park, J. Y.; Choi, C. S.; Cho, S. H.; Lee, J. L.:

"Enhanced Black State Induced by Spatial Silver Nanoparticles in an Electrochromic Device", NPG Asia Mater 9, 3 (2017)
30) Hou, X.; Wang, Z.; Zheng, Z.; Guo, J.; Sun, Z.; Yan, F.: "Poly(Ionic Liquid) Electrolytes for a Switchable Silver Mirror", ACS Appl Mater Interfaces 11, 22, pp.20417-20424 (June 5, 2019)
31) Bhoumik, N. C.; Madu, D. C.; Moon, C. W.; Arvisu, L. S.; McGehee, M. D.; Barile, C. J.: "Nonaqueous Electrolytes for Reversible Zinc Electrodeposition for Dynamic Windows with Excellent Optical Contrast and Durability", Joule 8, 4, pp.1036-1049 (Apr. 17, 2024)
32) Eh, A.L. S.; Lin, M. F.; Cui, M.; Cai, G.; Lee, P. S.: "A Copper-Based Reversible Electrochemical Mirror Device with Switchability between Transparent, Blue and Mirror States", J Mater Chem C Mater 5, 26, pp.6547-6554 (2017)
33) Chrdoba De Torresi ‘, S. I.; Carlos, I. A.: "Optical Characterization of Bismuth Reversible Electrodeposition", Journal of Electroanalytical Chemistry 414, , pp.1-16 (1996)
34) Imamura, A.; Kimura, M.; Kon, T.; Sunohara, S.; Kobayashi, N.: "Bi-Based Electrochromic Cell with Mediator for White/Black Imaging", Solar Energy Materials and Solar Cells 93, 12, pp.2079-2082 (Dec. 2009)
35) Araki, S.; Nakamura, K.; Kobayashi, K.; Tsuboi, A.; Kobayashi, N.: "Electrochemical Optical-Modulation Device with Reversible Transformation between Transparent, Mirror and Black", Advanced Materials 24, 23 (June 19, 2012)
36) Cho, S. M.; Kim, S.; Kim, T. Y.; Ah, C. S.; Song, J.; Cheon, S. H.; Kim, J. Y.; Ryu, H.; Kim, Y. H.; Hwang, C. S.; Lee, J. I.: "New Switchable Mirror Device with a Counter Electrode Based on Reversible Electrodeposition", Solar Energy Materials and Solar Cells 179, , pp.161-168 (June 1, 2018)
37) Park, C.; Seo, S.; Shin, H.; Sarwade, B. D.; Na, J.; Kim, E.: "Switchable Silver Mirrors with Long Memory Effects", Chem Sci 6, 1, pp.596-602 (Jan. 1, 2015)
38) Bhoumik, N. C.; Potts, C. R.; Hernandez, T. S.; Barile, C. J.: "Enhancing the Dark-State Bistability and Thermal Stability of Zinc Dynamic Windows with Nitrile Electrolytes", Device 2, 8, pp.100412 (Aug. 2024)
39) Bhoumik, N. C.; Thompson, S. M.; Barile, C. J.: "Electrolyte Design for Zinc Dynamic Windows with Fast Switching That Cycle More than 11, 000 Times with High Optical Contrast", Nano Energy 126, , pp.109710 (July 2024)
40) Kimura, S.; Sugita, T.; Nakamura, K.; Kobayashi, N.: "An Improvement in the Coloration Properties of Ag Deposition-Based Plasmonic EC Devices by Precise Control of Shape and Density of Deposited Ag Nanoparticles", Nanoscale 12, 47, pp.23975-23983 (Dec. 21, 2020)
41) Tsuboi, A.; Nakamura, K.; Kobayashi, N.: "Chromatic Control of Multicolor Electrochromic Device with Localized Surface Plasmon Resonance of Silver Nanoparticles by Voltage-Step Method", Solar Energy Materials and Solar Cells 145, , pp.16-25 (Feb. 1, 2016)
42) Tsuboi, A.; Nakamura, K.; Kobayashi, N.: "Chromatic Characterization of Novel Multicolor Reflective Display with Electrochemically Size-Controlled Silver Nanoparticles", J Soc Inf Disp 21, 8, pp.361-367 (Aug. 2013)
43) Tsuboi, A.; Nakamura, K.; Kobayashi, N.: "Multicolor Electrochromism Showing Three Primary Color States (Cyan-Magenta-Yellow) Based on Size- and Shape-Controlled Silver Nanoparticles", Chemistry of Materials 26, 22, pp.6477-6485 (Nov. 25, 2014)
44) Tsuboi, A.; Nakamura, K.; Kobayashi, N.: "A Localized Surface Plasmon Resonance-Based Multicolor Electrochromic Device with Electrochemically Size-Controlled Silver Nanoparticles", Advanced Materials 25, 23, pp.3197-3201 (June 2013)
45) Uji, S.; Kimura, S.; Nakamura, K.; Kobayashi, N.: "Analysis for Coloration Mechanism of Reversible Silver Deposition-Based Electrochromic Device by in Situ Observation of Plasmonic Nanoparticles with Dark-Field Microscopy", Solar Energy Materials and Solar Cells 251, (Mar. 1, 2023)
46) Onodera, R.; Tsuboi, A.; Nakamura, K.; Kobayashi, N.: "Coloration Mechanisms of Ag Deposition-Based Multicolor Electrochromic Device Investigated by Morphology of Ag Deposit and Its Optical Properties", J Soc Inf Disp 24, 7, pp.424-432 (July 1, 2016)
47) Uji, S.; Kon, T.; Mizuguchi, K.; Nakamura, K.; Kobayashi, N.: "Control of Ag Deposition for Improvement of Specular Reflection in Ag Deposition-Based Electrochemical Mirror through Modulation of Electrolysis Condition", Solar Energy Materials and Solar Cells 276, (Oct. 1, 2024)
48) Evanoff, D. D.; Chumanov, G.: "Size-Controlled Synthesis of Nanoparticles. 1.: "Silver-Only" Aqueous Suspensions via Hydrogen Reduction", Journal of Physical Chemistry B 108, 37, pp.13948-13956 (Sep. 16, 2004)
49) Huang, T.; Xu, X.H. N.: "Synthesis and Characterization of Tunable Rainbow Colored Colloidal Silver Nanoparticles Using Single-Nanoparticle Plasmonic Microscopy and Spectroscopy", J Mater Chem 20, 44, pp.9867-9876 (Nov. 28, 2010)
50) Kazuma, E.; Yamaguchi, T.; Sakai, N.; Tatsuma, T.: "Growth Behaviour and Plasmon Resonance Properties of Photocatalytically Deposited Cu Nanoparticles", Nanoscale 3, 9, pp.3641-3645 (Sep. 2011)
51) Kimura, S.; Wakatsuki, H.; Nakamura, K.; Kobayashi, N.: "Compensative Electrochromic Device Utilizing Electro-Deposited Plasmonic Silver Nanoparticles and Manganese Oxide to Achieve Retention of Chromatic Color", Electrochemistry 90, 4 (2022)
52) Uji, S.; Nakamura, K.; Kobayashi, N.: "The Effect of a Polymer Capping Agent on Electrodeposited Silver Nanoparticles in a Silver Deposition-Based Electrochromic Device", Physical Chemistry Chemical Physics 26, 23, pp.16466-16476 (Mar. 22, 2024)
53) Uji, S.; Nakamura, K.; Kobayashi, N.: "Dynamic Coloration Switching of Electrochemically Synthesized Silver Nanoparticles on the ITO Electrode Using a Polymer Capping Agent", Chem Lett 53, 11 (Nov. 5, 2024)
54) Dozol, H.; Mériguet, G.; Ancian, B.; Cabuil, V.; Xu, H.; Wang, D.; Abou-Hassan, A.: "On the Synthesis of Au Nanoparticles Using EDTA as a Reducing Agent", Journal of Physical Chemistry C 117, 40, pp.20958-20966 (Oct. 10, 2013)
55) Nakayama, T.; Honda, R.: "Electrochemical and Mechanistic Study of Superoxide Elimination by Mesalazine through Proton-Coupled Electron Transfer", Pharmaceuticals 14, 2, pp.1-12 (Feb. 1, 2021)
56) Fojtik, A.; Czapski, G.; Henglein, A.: "Pulse Radiolytic Investigation of the Carboxyl Radical in Aqueous Solution", J Phys Chem 74, 17, pp.3204-3208 (Aug. 1, 1970)
57) Antony Jeevarajan; Richard W. Fessenden.: "ESR Study of the Photochemistry of Benzoic Acid Derivatives", J Am Chem Soc 114, 26, pp.10461-10470 (Dec. 1992)
58) Johannsmann, D.; Reviakine, I.; Richter, R. P.: "Dissipation in Films of Adsorbed Nanospheres Studied by Quartz Crystal Microbalance (QCM)", Anal Chem 81, 19, pp.8167-8176 (Oct. 1, 2009)

Shun Uji received M.E. and Ph.D. degrees from Chiba University, Japan, in 2022 and 2025, respectively. His current research interest is focused on the fusion of electrochemistry and imaging at the Extreme Ultraviolet (EUV) region. In particular, he specializes in the analysis of metal deposition processes using EUV microscopy. Now, he works at Tokyo Polytechnic University as a postdoctoral scholar.

Kotaro Umetani entered the M.E. program at the Graduate School of Science and Engineering, Chiba University in 2025. His research interest is focused on electrochromic displays.

"Enhanced Black State Induced by Spatial Silver Nanoparticles in an Electrochromic Device", NPG Asia Mater 9, 3 (2017)
30) Hou, X.; Wang, Z.; Zheng, Z.; Guo, J.; Sun, Z.; Yan, F.: "Poly(Ionic Liquid) Electrolytes for a Switchable Silver Mirror", ACS Appl Mater Interfaces 11, 22, pp.20417-20424 (June 5, 2019)
31) Bhoumik, N. C.; Madu, D. C.; Moon, C. W.; Arvisu, L. S.; McGehee, M. D.; Barile, C. J.: "Nonaqueous Electrolytes for Reversible Zinc Electrodeposition for Dynamic Windows with Excellent Optical Contrast and Durability", Joule 8, 4, pp.1036-1049 (Apr. 17, 2024)
32) Eh, A.L. S.; Lin, M. F.; Cui, M.; Cai, G.; Lee, P. S.: "A Copper-Based Reversible Electrochemical Mirror Device with Switchability between Transparent, Blue and Mirror States", J Mater Chem C Mater 5, 26, pp.6547-6554 (2017)
33) Chrdoba De Torresi ', S. I.; Carlos, I. A.: "Optical Characterization of Bismuth Reversible Electrodeposition", Journal of Electroanalytical Chemistry 414, , pp.1-16 (1996)
34) Imamura, A.; Kimura, M.; Kon, T.; Sunohara, S.; Kobayashi, N.: "Bi-Based Electrochromic Cell with Mediator for White/Black Imaging", Solar Energy Materials and Solar Cells 93, 12, pp.2079-2082 (Dec. 2009)
35) Araki, S.; Nakamura, K.; Kobayashi, K.; Tsuboi, A.; Kobayashi, N.: "Electrochemical Optical-Modulation Device with Reversible Transformation between Transparent, Mirror and Black", Advanced Materials 24, 23 (June 19, 2012)
36) Cho, S. M.; Kim, S.; Kim, T. Y.; Ah, C. S.; Song, J.; Cheon, S. H.; Kim, J. Y.; Ryu, H.; Kim, Y. H.; Hwang, C. S.; Lee, J. I.: "New Switchable Mirror Device with a Counter Electrode Based on Reversible Electrodeposition", Solar Energy Materials and Solar Cells 179, , pp.161-168 (June 1, 2018)
37) Park, C.; Seo, S.; Shin, H.; Sarwade, B. D.; Na, J.; Kim, E.: "Switchable Silver Mirrors with Long Memory Effects", Chem Sci 6, 1, pp.596-602 (Jan. 1, 2015)
38) Bhoumik, N. C.; Potts, C. R.; Hernandez, T. S.; Barile, C. J.: "Enhancing the Dark-State Bistability and Thermal Stability of Zinc Dynamic Windows with Nitrile Electrolytes", Device 2, 8, pp.100412 (Aug. 2024)
39) Bhoumik, N. C.; Thompson, S. M.; Barile, C. J.: "Electrolyte Design for Zinc Dynamic Windows with Fast Switching That Cycle More than 11, 000 Times with High Optical Contrast", Nano Energy 126, , pp.109710 (July 2024)
40) Kimura, S.; Sugita, T.; Nakamura, K.; Kobayashi, N.: "An Improvement in the Coloration Properties of Ag Deposition-Based Plasmonic EC Devices by Precise Control of Shape and Density of Deposited Ag Nanoparticles", Nanoscale 12, 47, pp.23975-23983 (Dec. 21, 2020)
41) Tsuboi, A.; Nakamura, K.; Kobayashi, N.: "Chromatic Control of Multicolor Electrochromic Device with Localized Surface Plasmon Resonance of Silver Nanoparticles by Voltage-Step Method", Solar Energy Materials and Solar Cells 145, , pp.16-25 (Feb. 1, 2016)
42) Tsuboi, A.; Nakamura, K.; Kobayashi, N.: "Chromatic Characterization of Novel Multicolor Reflective Display with Electrochemically Size-Controlled Silver Nanoparticles", J Soc Inf Disp 21, 8, pp.361-367 (Aug. 2013)
43) Tsuboi, A.; Nakamura, K.; Kobayashi, N.: "Multicolor Electrochromism Showing Three Primary Color States (Cyan-Magenta-Yellow) Based on Size- and Shape-Controlled Silver Nanoparticles", Chemistry of Materials 26, 22, pp.6477-6485 (Nov. 25, 2014)
44) Tsuboi, A.; Nakamura, K.; Kobayashi, N.: "A Localized Surface Plasmon Resonance-Based Multicolor Electrochromic Device with Electrochemically Size-Controlled Silver Nanoparticles", Advanced Materials 25, 23, pp.3197-3201 (June 2013)
45) Uji, S.; Kimura, S.; Nakamura, K.; Kobayashi, N.: "Analysis for Coloration Mechanism of Reversible Silver Deposition-Based Electrochromic Device by in Situ Observation of Plasmonic Nanoparticles with Dark-Field Microscopy", Solar Energy Materials and Solar Cells 251, (Mar. 1, 2023)
46) Onodera, R.; Tsuboi, A.; Nakamura, K.; Kobayashi, N.: "Coloration Mechanisms of Ag Deposition-Based Multicolor Electrochromic Device Investigated by Morphology of Ag Deposit and Its Optical Properties", J Soc Inf Disp 24, 7, pp.424-432 (July 1, 2016)
47) Uji, S.; Kon, T.; Mizuguchi, K.; Nakamura, K.; Kobayashi, N.: "Control of Ag Deposition for Improvement of Specular Reflection in Ag Deposition-Based Electrochemical Mirror through Modulation of Electrolysis Condition", Solar Energy Materials and Solar Cells 276, (Oct. 1, 2024)
48) Evanoff, D. D.; Chumanov, G.: "Size-Controlled Synthesis of Nanoparticles. 1.: "Silver-Only" Aqueous Suspensions via Hydrogen Reduction", Journal of Physical Chemistry B 108, 37, pp.13948-13956 (Sep. 16, 2004)
49) Huang, T.; Xu, X.H. N.: "Synthesis and Characterization of Tunable Rainbow Colored Colloidal Silver Nanoparticles Using Single-Nanoparticle Plasmonic Microscopy and Spectroscopy", J Mater Chem 20, 44, pp.9867-9876 (Nov. 28, 2010)
50) Kazuma, E.; Yamaguchi, T.; Sakai, N.; Tatsuma, T.: "Growth Behaviour and Plasmon Resonance Properties of Photocatalytically Deposited Cu Nanoparticles", Nanoscale 3, 9, pp.3641-3645 (Sep. 2011)
51) Kimura, S.; Wakatsuki, H.; Nakamura, K.; Kobayashi, N.: "Compensative Electrochromic Device Utilizing Electro-Deposited Plasmonic Silver Nanoparticles and Manganese Oxide to Achieve Retention of Chromatic Color", Electrochemistry 90, 4 (2022)
52) Uji, S.; Nakamura, K.; Kobayashi, N.: "The Effect of a Polymer Capping Agent on Electrodeposited Silver Nanoparticles in a Silver Deposition-Based Electrochromic Device", Physical Chemistry Chemical Physics 26, 23, pp.16466-16476 (Mar. 22, 2024)
53) Uji, S.; Nakamura, K.; Kobayashi, N.: "Dynamic Coloration Switching of Electrochemically Synthesized Silver Nanoparticles on the ITO Electrode Using a Polymer Capping Agent", Chem Lett 53, 11 (Nov. 5, 2024)
54) Dozol, H.; Mériguet, G.; Ancian, B.; Cabuil, V.; Xu, H.; Wang, D.; Abou-Hassan, A.: "On the Synthesis of Au Nanoparticles Using EDTA as a Reducing Agent", Journal of Physical Chemistry C 117, 40, pp.20958-20966 (Oct. 10, 2013)
55) Nakayama, T.; Honda, R.: "Electrochemical and Mechanistic Study of Superoxide Elimination by Mesalazine through Proton-Coupled Electron Transfer", Pharmaceuticals 14, 2, pp.1-12 (Feb. 1, 2021)
56) Fojtik, A.; Czapski, G.; Henglein, A.: "Pulse Radiolytic Investigation of the Carboxyl Radical in Aqueous Solution", J Phys Chem 74, 17, pp.3204-3208 (Aug. 1, 1970)
57) Antony Jeevarajan; Richard W. Fessenden.: "ESR Study of the Photochemistry of Benzoic Acid Derivatives", J Am Chem Soc 114, 26, pp.10461-10470 (Dec. 1992)
58) Johannsmann, D.; Reviakine, I.; Richter, R. P.: "Dissipation in Films of Adsorbed Nanospheres Studied by Quartz Crystal Microbalance (QCM)", Anal Chem 81, 19, pp.8167-8176 (Oct. 1, 2009)

Shun Uji received M.E. and Ph.D. degrees from Chiba University, Japan, in 2022 and 2025, respectively. His current research interest is focused on the fusion of electrochemistry and imaging at the Extreme Ultraviolet (EUV) region. In particular, he specializes in the analysis of metal deposition processes using EUV microscopy. Now, he works at Tokyo Polytechnic University as a postdoctoral scholar.

Kotaro Umetani entered the M.E. program at the Graduate School of Science and Engineering, Chiba University in 2025. His research interest is focused on electrochromic displays.

Nikhil C. Bhoumik received his B.Sc. (Hons.), M.S., and M.Phil. degrees in Chemistry from Jahangirnagar University, Bangladesh. He is currently pursuing his Ph.D. in Chemistry at the University of Nevada, Reno, USA. His research focuses on electrochemical energy storage, electrocatalysis, and functional materials. He has authored publications in Joule, Nano Energy, and Angewandte Chemie, and holds a U.S. patent on nonaqueous zinc-based dynamic windows. His recent work includes the development of novel electrolytes, reversible metal electrodeposition systems, and catalysts for CO_2 reduction, oxygen reduction reaction (ORR), nitrogen reduction reaction (N_2RR), and other sustainable electrochemical transformations.

Kazuki Nakamura in March 2007, he received his PhD from Graduate School of Engineering, Osaka University, Japan. From 2007 to 2009, he worked at Advanced Technology R & D Center, Mitsubishi Electric Corporation. Since April 2009 he worked as Assistant Professor in Graduate School of Advanced Integration Science, Chiba University. He was promoted to Associate Professor in July 2015 at the same department. In 2017, the school was reorganized into the Graduate School of Engineering, where he continued his appointment. Then, he was appointed Professor in October 2023. He has been a member of the editorial board of the Imaging Society of Japan since 2011, and served as Editor-in-Chief from 2018 to 2022. Since 2020, he has also been serving as a member of the organizing committee (in charge of the secretariat) of the Photofunctional Complexes Research Association Japan. His research interest is focused on stimuli-responsive photoelectronic functional materials especially based on lanthanide(III) compounds.

Christopher J. Barile holds the Clemons-Magee Professorship in the Department of Chemistry at the University of Nevada, Reno. He received his BSc with distinction and a co-terminal MSc in chemistry from Stanford University. He went on to earn his PhD at the University of Illinois at Urbana-Champaign, where he focused on developing next-generation battery technologies. Following his doctorate, Prof. Barile returned to Stanford as a postdoctoral scholar in materials science and engineering before beginning his independent research career in 2017. His work spans electrochemistry, inorganic chemistry, and materials chemistry, with a focus on addressing challenges in energy conversion, storage, and efficiency.

Norihisa Kobayashi received his PhD in 1988 from Waseda University, Japan. He worked as Assistant Professor in Department of Image Science, Chiba University (1987-1995). He was also Visiting Associate, California Institute of Technology, USA (1992-1993), He has worked as a Associate professor in Department of Image Science, Chiba University (1995-2004). Since 2004, he held a position of professor in current position of Graduate School of Engineering. Chiba University. His research interest primarily focused on photoelectronic-functional molecules including polymer for development of photoconductive materials, materials with high electronic carrier mobility, highly emissive materials, light emitting materials, ionic conductive materials, electroactive materials, chromogenic materials and so on.

Nikhil C. Bhoumik received his B.Sc. (Hons.), M.S., and M.Phil. degrees in Chemistry from Jahangirnagar University, Bangladesh. He is currently pursuing his Ph.D. in Chemistry at the University of Nevada, Reno, USA. His research focuses on electrochemical energy storage, electrocatalysis, and functional materials. He has authored publications in Joule, Nano Energy, and Angewandte Chemie, and holds a U.S. patent on nonaqueous zinc-based dynamic windows. His recent work includes the development of novel electrolytes, reversible metal electrodeposition systems, and catalysts for CO_2 reduction, oxygen reduction reaction (ORR), nitrogen reduction reaction (N_2RR), and other sustainable electrochemical transformations.

Kazuki Nakamura in March 2007, he received his PhD from Graduate School of Engineering, Osaka University, Japan. From 2007 to 2009, he worked at Advanced Technology R & D Center, Mitsubishi Electric Corporation. Since April 2009 he worked as Assistant Professor in Graduate School of Advanced Integration Science, Chiba University. He was promoted to Associate Professor in July 2015 at the same department. In 2017, the school was reorganized into the Graduate School of Engineering, where he continued his appointment. Then, he was appointed Professor in October 2023. He has been a member of the editorial board of the Imaging Society of Japan since 2011, and served as Editor-in-Chief from 2018 to 2022. Since 2020, he has also been serving as a member of the organizing committee (in charge of the secretariat) of the Photofunctional Complexes Research Association Japan. His research interest is focused on stimuli-responsive photoelectronic functional materials especially based on lanthanide(III) compounds.

Christopher J. Barile holds the Clemons-Magee Professorship in the Department of Chemistry at the University of Nevada, Reno. He received his BSc with distinction and a co-terminal MSc in chemistry from Stanford University. He went on to earn his PhD at the University of Illinois at Urbana-Champaign, where he focused on developing next-generation battery technologies. Following his doctorate, Prof. Barile returned to Stanford as a postdoctoral scholar in materials science and engineering before beginning his independent research career in 2017. His work spans electrochemistry, inorganic chemistry, and materials chemistry, with a focus on addressing challenges in energy conversion, storage, and efficiency.

Norihisa Kobayashi received his PhD in 1988 from Waseda University, Japan. He worked as Assistant Professor in Department of Image Science, Chiba University (1987-1995). He was also Visiting Associate, California Institute of Technology, USA (1992-1993), He has worked as a Associate professor in Department of Image Science, Chiba University (1995-2004). Since 2004, he held a position of professor in current position of Graduate School of Engineering. Chiba University. His research interest primarily focused on photoelectronic-functional molecules including polymer for development of photoconductive materials, materials with high electronic carrier mobility, highly emissive materials, light emitting materials, ionic conductive materials, electroactive materials, chromogenic materials and so on.